Innate lymphoid cells and disease tolerance in SARS-CoV-2 infection

Noah J. Silverstein[1,2,3*], Yetao Wang[1,3*], Zachary Manickas-Hill[3,4], Claudia Carbone[1], Ann Dauphin[1], Brittany P. Boribong[5,6,7], Maggie Loiselle[5], Jameson Davis[5], Maureen M. Leonard[5,6,7], Leticia Kuri-Cervantes[8,9], MGH COVID-19 Collection & Processing Team, Nuala J. Meyer[10], Michael R. Betts[8,9], Jonathan Z. Li[3,11], Bruce Walker[3,4,12,13], Xu G. Yu[3,4,11], Lael M. Yonker[5,6,7], Jeremy Luban[1,3,14,15]

[1]Program in Molecular Medicine, University of Massachusetts Medical School, Worcester, MA 01605, USA
[2]Medical Scientist Training Program, University of Massachusetts Medical School, Worcester, MA 01605, USA
[3]Massachusetts Consortium on Pathogen Readiness, Boston, MA, 02115
[4]Ragon Institute of MGH, MIT and Harvard, Cambridge, MA 02139, USA
[5]Massachusetts General Hospital, Mucosal Immunology and Biology Research Center, Boston, MA, USA
[6]Massachusetts General Hospital, Department of Pediatrics, Boston, MA, USA
[7]Harvard Medical School, Boston, MA, USA
[8]Department of Microbiology, Perelman School of Medicine, University of Pennsylvania, Philadelphia, PA 19104, USA
[9]Institute for Immunology, Perelman School of Medicine, University of Pennsylvania, Philadelphia, PA 19104, USA.
[10]Division of Pulmonary and Critical Care Medicine, Department of Medicine, University of Pennsylvania Perelman School of Medicine, Philadelphia, PA 19104, USA
[11]Department of Medicine, Brigham and Women's Hospital, Boston, MA 02115, USA
[12]Howard Hughes Medical Institute, Chevy Chase, MD 20815, USA
[13]Department of Biology and Institute of Medical Engineering and Science, Massachusetts Institute of Technology, Cambridge, MA
[14]Department of Biochemistry and Molecular Pharmacology, University of Massachusetts Medical School, Worcester, MA 01605, USA
[15]Broad Institute of Harvard and MIT, 75 Ames Street, Cambridge, MA 02142, USA

*These authors contributed equally

Correspondence: yetao.wang@umassmed.edu (Y.W.); jeremy.luban@umassmed.edu (J.L.)

Abstract:

Risk of severe COVID-19 increases with age, is greater in males, and is associated with lymphopenia, but not with higher burden of SARS-CoV-2. It is unknown whether effects of age and sex on abundance of specific lymphoid subsets explain these correlations. This study found that the abundance of innate lymphoid cells (ILCs) decreases more than 7-fold over the human lifespan — T cell subsets decrease less than 2-fold — and is lower in males than in females. After accounting for effects of age and sex, ILCs, but not T cells, were lower in adults hospitalized with COVID-19, independent of lymphopenia. Among SARS-CoV-2-infected adults, the abundance of ILCs, but not of T cells, correlated inversely with odds and duration of hospitalization, and with severity of inflammation. ILCs were also uniquely decreased in pediatric COVID-19 and the numbers of these cells did not recover during follow-up. In contrast, children with MIS-C had depletion of both ILCs and T cells, and both cell types increased during follow-up. In both pediatric COVID-19 and MIS-C, ILC abundance correlated inversely with inflammation. Blood ILC mRNA and phenotype tracked closely with ILCs from lung. Importantly, blood ILCs produced amphiregulin, a protein implicated in disease tolerance and tissue homeostasis, and the percentage of amphiregulin-producing ILCs was higher in females than in males. These results suggest that, by promoting disease tolerance, homeostatic ILCs decrease morbidity and mortality associated with SARS-CoV-2 infection, and that lower ILC abundance accounts for increased COVID-19 severity with age and in males.

INTRODUCTION

The risk of severe COVID-19 and death in people infected with SARS-CoV-2 increases with age and is greater in men than in women (Alkhouli et al., 2020; Bunders and Altfeld, 2020; Gupta et al., 2021; Laxminarayan et al., 2020; Mauvais-Jarvis, 2020; O'Driscoll et al., 2020; Peckham et al., 2020; Richardson et al., 2020; Scully et al., 2020). These trends have been observed in people infected with SARS-CoV (Chen and Subbarao, 2007; Donnelly et al., 2003; Karlberg, 2004), or with MERS-CoV (Alghamdi et al., 2014), and in laboratory animals challenged with SARS-CoV or SARS-CoV-2 (Channappanavar et al., 2017; Leist et al., 2020). Yet, the mechanisms underlying these effects of age and sex on COVID-19 morbidity and mortality remain poorly understood.

The composition and function of the human immune system changes with age and exhibits sexual dimorphism (Darboe et al., 2020; Klein and Flanagan, 2016; Márquez et al., 2020; Patin et al., 2018; Solana et al., 2012), with consequences for survival of infection, response to vaccination, and susceptibility to autoimmune disease (Flanagan et al., 2017; Giefing-Kröll et al., 2015; Márquez et al., 2020; Mauvais-Jarvis, 2020; Patin et al., 2018; Piasecka et al., 2018). Better understanding of these effects might provide clues as to why the clinical outcome of SARS-CoV-2 infection is so variable, ranging from asymptomatic to lethal (Cevik et al., 2021; He et al., 2021; Jones et al., 2021; Lee et al., 2020; Lennon et al., 2020; Ra et al., 2021; Richardson et al., 2020; Yang et al., 2021).

Survival after infection with a pathogenic virus such as SARS-CoV-2 requires not only that the immune system control and eliminate the pathogen, but that disease tolerance mechanisms limit tissue damage caused by the pathogen or by host inflammatory responses (Ayres, 2020a; McCarville and Ayres, 2018; Medzhitov et al.,

85 2012; Schneider and Ayres, 2008). Research with animal models has demonstrated that
86 genetic and environmental factors can promote host fitness without directly inhibiting
87 pathogen replication (Ayres, 2020a; Cumnock et al., 2018; Jhaveri et al., 2007; McCarville
88 and Ayres, 2018; Medzhitov et al., 2012; Råberg et al., 2007; Sanchez et al., 2018;
89 Schneider and Ayres, 2008; Wang et al., 2016). Although in most cases the underlying
90 mechanism is unknown, some of these models suggest that subsets of innate lymphoid
91 cells (ILCs) contribute to disease tolerance (Artis and Spits, 2015; Branzk et al., 2018;
92 Califano et al., 2018; Diefenbach et al., 2020; McCarville and Ayres, 2018; Monticelli et
93 al., 2015, 2011).

94 ILCs lack clonotypic antigen receptors but overlap developmentally and
95 functionally with T cells. Based on expression of characteristic transcription factors and
96 specific inducible cytokines, ILCs are classified into ILC1, ILC2, and ILC3 subsets that
97 are analogous to T_H1, T_H2, and T_H17 cells respectively (Artis and Spits, 2015; Cherrier et
98 al., 2018; Vivier et al., 2018; Yudanin et al., 2019). Additionally, some ILC subsets
99 produce the epidermal growth factor family member amphiregulin (AREG) that maintains
100 the integrity of epithelial barriers in the lung and intestine (Branzk et al., 2018; Jamieson
101 et al., 2013; Monticelli et al., 2015, 2011), and promotes tissue repair (Artis and Spits,
102 2015; Cherrier et al., 2018; Klose and Artis, 2016; Rak et al., 2016). In models of influenza
103 infection in mice, homeostatic ILCs and exogenous AREG promote lung epithelial
104 integrity, decrease disease severity, and increase survival, without decreasing pathogen
105 burden (Califano et al., 2018; Jamieson et al., 2013; Monticelli et al., 2011).

106 Little is known about disease tolerance in the context of human infectious
107 diseases. Interestingly, SARS-CoV-2 viral load does not reliably discriminate

108 symptomatic from asymptomatic infection (Cevik et al., 2021; Jones et al., 2021; Lee et
109 al., 2020; Lennon et al., 2021; Ra et al., 2021; Yang et al., 2021). This discrepancy
110 between SARS-CoV-2 viral load and the severity of COVID-19 is especially pronounced
111 in children, who rarely have severe COVID-19 (Charles Bailey et al., 2020; Li et al., 2020;
112 Lu et al., 2020; Poline et al., 2020), though viral load may be comparable to that in adults
113 with severe COVID-19 (Heald-Sargent et al., 2020; LoTempio et al., 2021; Yonker et al.,
114 2020). These observations suggest that age-dependent, disease tolerance mechanisms
115 influence the severity of COVID-19. In mice, homeostatic ILCs decrease in abundance in
116 the lung with increasing age, and lose their ability to maintain disease tolerance during
117 influenza infection (D'Souza et al., 2019). Although the distribution of ILCs within human
118 tissues differs from mice and is heterogeneous among individuals (Yudanin et al., 2019),
119 human ILCs share many features with those in mice (Vivier et al., 2018) and therefore
120 likely perform similar roles in maintaining tissue homeostasis and disease tolerance.

121 ILCs in peripheral blood have been reported to be depleted in individuals with
122 severe COVID-19 (García et al., 2020; Kuri-Cervantes et al., 2020), but it is difficult to
123 determine the extent to which ILCs are decreased independently from the overall
124 lymphopenia associated with COVID-19 (Chen et al., 2020; Huang et al., 2020; Huang
125 and Pranata, 2020; Zhang et al., 2020; Zhao et al., 2020), or from the reported decreases
126 in other blood lymphoid cell populations (Kuri-Cervantes et al., 2020; Lucas et al., 2020;
127 Mathew et al., 2020; Mudd et al., 2020; Zheng et al., 2020). In addition, assessment of
128 lymphoid cell abundance, in the context of a disease for which age and sex are risk factors
129 for severity, is confounded by programmed differences in lymphocyte abundance with
130 age and sex (Márquez et al., 2020; Patin et al., 2018). The goal of this study was to

131 determine whether the abundance of any blood lymphoid cell population was altered in
132 COVID-19, independent of age, sex, and global lymphopenia, and whether abundance of
133 any lymphoid cell population correlated with clinical outcome in SARS-CoV-2 infection.

134 # RESULTS

135 **Characteristics of adult blood donors hospitalized for COVID-19, treated for COVID-**
136 **19 as outpatients, or SARS-CoV-2-uninfected controls**

137 The first group of blood donors in this study included SARS-CoV-2-infected adults
138 hospitalized for severe COVID-19 (N = 40), among whom 33 (82.5%) were admitted to
139 the ICU, 32 (80%) required intubation with mechanical ventilation, and 7 (17.5%) died
140 (Table 1). This group had a mean age of 57.6 (range 24 to 83) and 60% were males. The
141 second group consisted of adults infected with SARS-CoV-2 who were treated for COVID-
142 19 as outpatients (N=51). This group had a mean age of 36.8 years (range 23-77) and
143 was 25.5% male (Table 1). Differences between these two SARS-CoV-2-infected groups,
144 in terms of median age ($p = 5.2 \times 10^{-8}$) and sex ratio ($p = 3.7 \times 10^{-3}$) (Fig. 1), were
145 consistent with the established greater risk of severe COVID-19 in older individuals and
146 in males (Alkhouli et al., 2020; Bunders and Altfeld, 2020; Gupta et al., 2021;
147 Laxminarayan et al., 2020; Mauvais-Jarvis, 2020; O'Driscoll et al., 2020; Peckham et al.,
148 2020; Richardson et al., 2020; Scully et al., 2020). Available information concerning
149 ethnicity and race of the blood donors was insufficient for statistical comparisons among
150 the groups (Supplementary Table S1). Finally, 86 adults who donated blood prior to the
151 SARS-CoV-2 outbreak, or who were screened at a blood donation center, were included
152 as controls for SARS-CoV-2 infection. The age of this group spanned the range of the
153 two groups of SARS-CoV-2-infected people (mean age 50.9; range 23 to 79), and the
154 percentage of males (55.8%) was similar to that of the group hospitalized for COVID-19
155 (Table 1 and Fig. 1).

156

Table 1: Demographic and Clinical Characteristics of Adult Blood Donor Groups

Characteristic	Healthy Control N=86	Hospitalized N=40	Outpatient N=51
Mean age (range) - years	50.9 (23-79)	57.6 (24-83)	36.8 (23-77)
Sex – number (%)			
Male	48 (55.8)	24 (60)	13 (25.5)
Female	38 (44.2)	16 (40)	38 (74.5)
Mean symptom duration at sample collection (range) – days		21.8 (5-66)	26.9 (1-61)
ICU admission – number (%)		33 (82.5)	
Intubation with mechanical ventilation – number (%)		32 (80)	
Deaths – number (%)		7 (17.5)	
Mean time hospitalized (range) – days		34.2 (4-87)	
Max lab value – mean (range)			
CRP – mg/L		228.6 (6.5-539.5)	
ESR – mm/h		89.0 (15-146)	
D-dimer – (ng/mL)		5700 (351-11923)	

157

158

159

160

161

162 **Characteristics of pediatric blood donors with COVID-19, MIS-C, or SARS-CoV-2-**
163 **uninfected controls**

164 Children are less likely than adults to have severe disease when infected with SARS-
165 CoV-2 despite having viral loads as high as adults (Charles Bailey et al., 2020; Heald-
166 Sargent et al., 2020; Li et al., 2020; LoTempio et al., 2021; Lu et al., 2020; Poline et al.,
167 2020; Yonker et al., 2020). Rarely, after SARS-CoV-2 clearance from the upper airways,
168 children can develop severe Multisystem Inflammatory Syndrome in Children (MIS-C), a
169 life-threatening condition distinct from COVID-19 that presents with high fevers and
170 multiorgan injury, often including coronary aneurysms, ventricular failure, or myocarditis
171 (Cheung et al., 2020; Feldstein et al., 2021, 2020; Licciardi et al., 2020; Riphagen et al.,
172 2020; Verdoni et al., 2020; Whittaker et al., 2020).

173 The first cohort of pediatric blood donors in this study consisted of patients with
174 COVID-19 who were treated in hospital (N=11) or as outpatients (N=8). The second
175 cohort of pediatric blood donors was patients hospitalized for MIS-C (N=11). Seventeen
176 SARS-CoV-2-uninfected pediatric blood donors constituted a control group. No significant
177 differences in age or percentage of males were detected among the pediatric COVID-19,
178 MIS-C, or pediatric control groups (Supplementary Table S2 and Fig. 1).

179

180

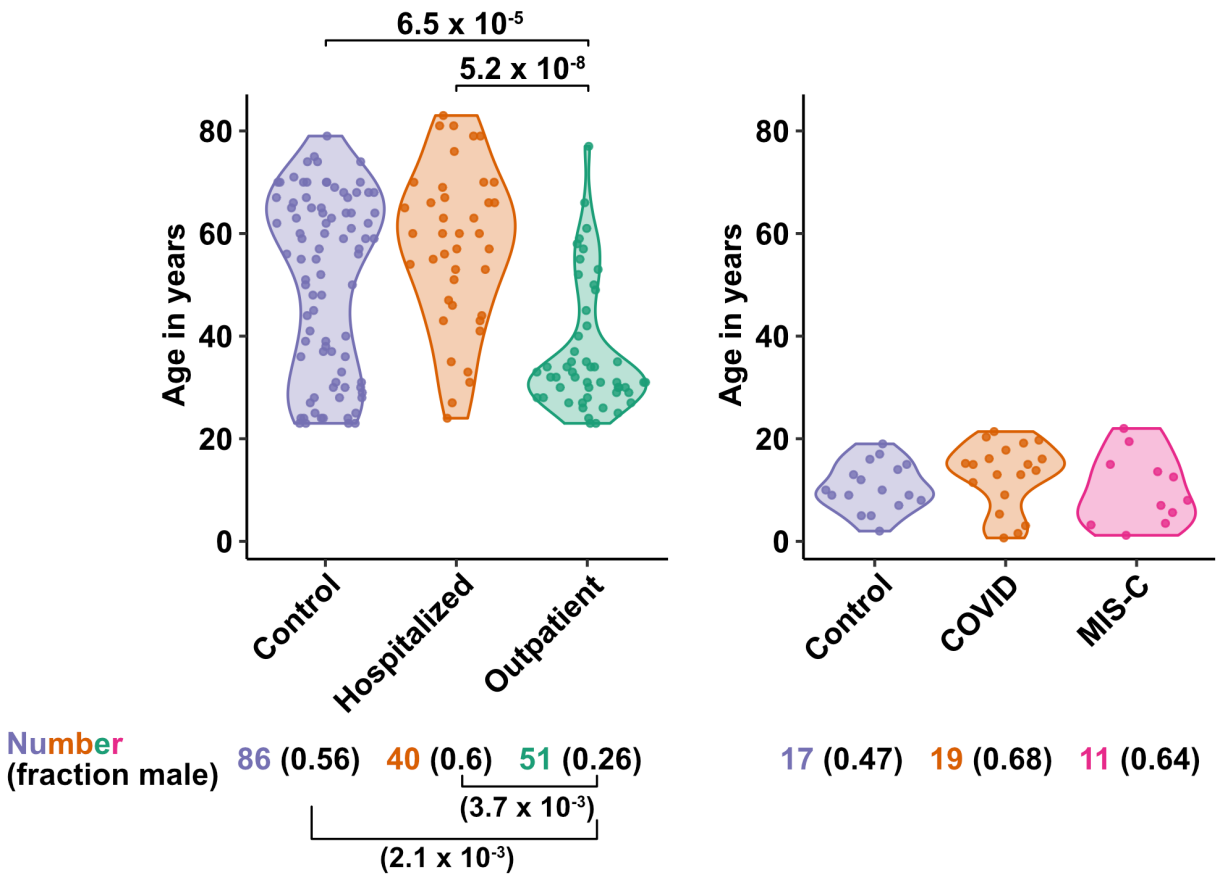

Fig. 1. Age and sex of control and SARS-CoV-2-infected blood donors

Age of the subjects is shown, along with the number of subjects and fraction male in each group, for adult (left) and pediatric (right) cohorts, as indicated. P-values are from pairwise, two-sided, Wilcoxon rank-sum test for ages and Fisher's exact test for fraction male, with Bonferroni correction for multiple comparisons. Adjusted P-values < 0.05 are shown.

192 **Blood ILC abundance decreases exponentially across the lifespan and is sexually**
193 **dimorphic**

194 Lymphoid cell abundance in peripheral blood changes with age and is sexually dimorphic
195 (Márquez et al., 2020; Patin et al., 2018). Previous studies reporting the effect of COVID-
196 19 on the abundance of blood lymphoid cell subsets have not fully accounted for the
197 association of age and sex with COVID-19 severity. To isolate the effect of COVID-19 on
198 cell abundance from effects of age and sex, PBMCs were collected from 103 SARS-CoV-
199 2-negative blood donors distributed from 2 to 79 years of age, with a nearly equal ratio of
200 males to females. Abundance of lymphoid cell types was plotted by 20-year age groups
201 (Fig. 2A), as well as by sex (Fig. 2B). Lymphoid cell types assessed here included $CD4^+$
202 T cells, $CD8^+$ T cells, ILCs, and FcγRIII (CD16)-positive NK cells. Like $CD8^+$ T cells, NK
203 cells kill virus-infected cells using perforin and granzyme (Artis and Spits, 2015; Cherrier
204 et al., 2018). Additionally, by binding virus-specific immunoglobulins that target virus-
205 infected cells for antibody-dependent cellular cytotoxicity, $CD16^+$ NK cells link innate and
206 acquired immunity (Anegon et al., 1988).

207 All cell types examined here were affected by age, but ILCs were the only subset
208 with significant differences among all age groups, falling approximately 2-fold in median
209 abundance every 20 years, with a greater than 7-fold decrease from the youngest to
210 oldest age groups ($p = 1.64 \times 10^{-11}$) (Fig. 2A). This magnitude of decrease was unique to
211 ILCs and corresponded inversely with the exponential increase in COVID-19 mortality
212 with age (O'Driscoll et al., 2020) (Fig. 2C). In addition, both ILCs and $CD4^+$ T cells were
213 less abundant in males (Fig. 2B). These findings highlight the importance of accounting
214 for effects of age and sex when assessing group differences in lymphoid cell abundance,

215 particularly in the context of a disease such as COVID-19 that disproportionately affects

216 older males (O'Driscoll et al., 2020).

217

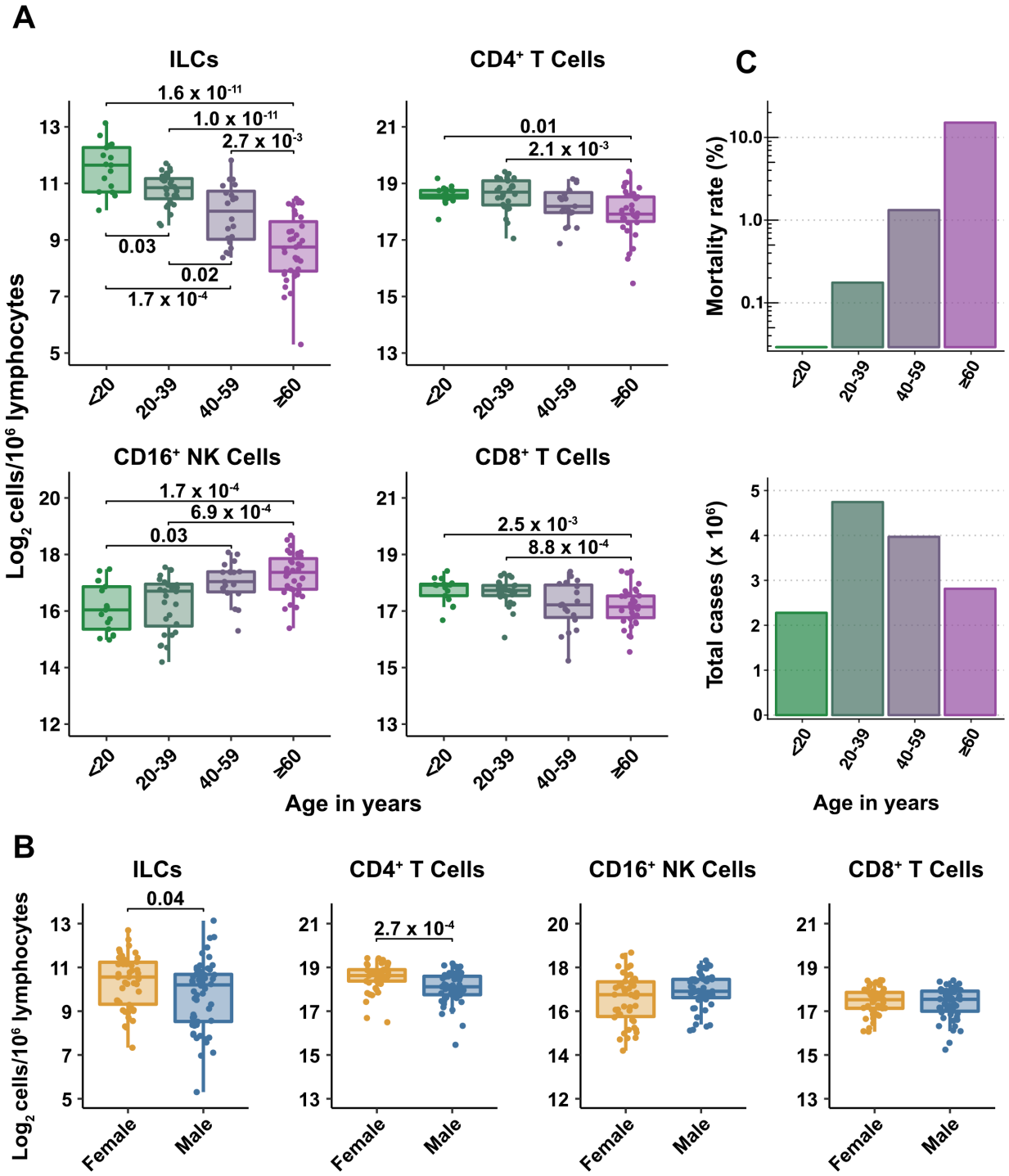

Fig. 2. Blood ILC abundance decreases exponentially across the lifespan mirroring the mortality rate from SARS-CoV-2 infection

221 (**A-B**) Log2 abundance per million lymphocytes of the indicated lymphoid cell populations
222 in combined pediatric and adult control data plotted by 20-year bin or by sex, as indicated.
223 Each dot represents an individual blood donor. Boxplots represent the distribution of the
224 data with the center line drawn through the median with the upper and lower bounds of
225 the box at the 75th and 25th percentiles respectively. The upper and lower whiskers
226 extend to the largest or smallest values within 1.5 x the interquartile range (IQR). P-values
227 are from two-sided, Wilcoxon rank-sum tests with Bonferroni correction for multiple
228 comparisons. Adjusted P-values < 0.05 are shown.
229 (**C**) Case numbers and mortality rate within the indicated age ranges for cases reported
230 in the United States between Jan 1, 2020, and June 6, 2021.
231
232
233
234
235
236
237
238
239
240
241
242
243

244 **Adults hospitalized with COVID-19 have fewer total lymphocytes even after**
245 **accounting for effects of age and sex**

246 Severe COVID-19 is associated with lymphopenia (Chen et al., 2020; Huang et al., 2020;
247 Huang and Pranata, 2020; Zhang et al., 2020; Zhao et al., 2020) but it remains unclear if
248 this effect is due to reduction in particular lymphoid cell subpopulations, or whether this
249 effect is explained by the more advanced age and higher proportion of males among
250 people with severe COVID-19. As a first step to assess the specificity of lymphocyte
251 depletion, the effect of COVID-19 on total lymphocyte abundance was addressed with
252 multiple linear regression. After accounting for effects of age and sex, individuals
253 hospitalized with severe COVID-19 had 1.33-fold (95%CI: 1.49–1.19; $p = 1.22 \times 10^{-6}$)
254 fewer total lymphocytes among PBMCs than did controls (Supplementary Table S3).
255 Lymphocyte abundance in people infected with SARS-CoV-2 who were treated as
256 outpatients was not different from controls (Supplementary Table S3). In addition, total
257 lymphocytes decreased with age and were less abundant in males (Supplementary Table
258 S3). Subsequent analyses of lymphoid cell subsets took into account the depletion in total
259 lymphocytes associated with COVID-19 by assessing lymphoid subsets as a fraction of
260 total lymphocytes.

261 **After accounting for age and sex, only innate lymphoid cells are depleted in severe**
262 **COVID-19**

263 To determine whether there were independent associations between lymphoid cell
264 subsets and COVID-19, multiple linear regression was performed on the abundance of
265 lymphoid cell subsets, with age, sex, and group (control, hospitalized, and outpatient) as
266 independent variables. Across all three groups of adult blood donors, $CD4^+$ T cells, $CD8^+$

267 T cells, and ILCs decreased with age, while CD16$^+$ NK cells increased with age, and both
268 CD4$^+$ T cells and ILCs were less abundant in males (Table 2 and Fig. 3A).
269

Table 2: Change in Cell Abundance Due to Age, Sex, and COVID-19 Severity

Fold difference (log2) [±95%CI]

	CD4$^+$ T^a	**ILC^a**	**CD8$^+$ T^a**	**CD16$^+$ NK^a**
Age	-0.012***	-0.043***	-0.009*	0.021***
	[-0.018, -0.005]	[-0.053, -0.033]	[-0.016, -0.002]	[0.010, 0.032]
Male	-0.409***	-0.334*	-0.177	0.184
	[-0.618, -0.201]	[-0.659, -0.010]	[-0.406, 0.051]	[-0.169, 0.538]
Hospitalized	0.168	-0.835***	0.227	-1.205***
	[-0.084, 0.421]	[-1.228, -0.441]	[-0.050, 0.503]	[-1.633, -0.778]
Outpatient	0.332*	-0.088	-0.023	-0.522*
	[0.082, 0.581]	[-0.478, 0.302]	[-0.298, 0.253]	[-0.948, -0.095]
R^2	0.275	0.478	0.070	0.232

* $p < 0.05$, ** $p < 0.01$, *** $p < 0.001$
^{a} per 10^6 lymphocytes

270

271 When effects of age and sex were held constant, adults hospitalized with COVID-
272 19 had 1.78-fold fewer ILCs (95%CI: 2.34–1.36; $p = 4.55 \times 10^{-5}$) and 2.31-fold fewer
273 CD16$^+$ natural killer (NK) cells (95%CI: 3.1–1.71; $p = 1.04 \times 10^{-7}$), as compared to controls
274 (Table 2 and Fig. 3B). Similar effects were also seen with ILC precursors (ILCP)
275 (Supplementary Fig. S1). Neither CD4$^+$ T cells nor CD8$^+$ T cells were depleted further
276 than expected for age and sex (Table 2 and Fig. 3B). As compared with controls, SARS-
277 CoV-2-infected adults with less severe COVID-19 who were treated as outpatients had

278 no reduction in ILCs, but 1.44-fold fewer $CD16^+$ NK cells (95%CI: 1.93–1.07; p = 0.018),
279 and 1.26-fold higher $CD4^+$ T cells (95%CI: 1.06–1.5; $p = 9.59 \times 10^{-3}$) (Table 2 and Fig.
280 3B). As these analyses were performed on lymphoid cell abundance normalized to total
281 lymphocyte number, it is possible that T cells were not lower in patients hospitalized with
282 COVID-19 because the amount of depletion was not in excess of the change in total
283 lymphocytes. However, the cell-type specific results remained unchanged even when the
284 analyses were repeated using the less stringent threshold of normalizing to total PBMC
285 number (Supplementary Table S4).

286 When data from an independent, previously published cohort (Kuri-Cervantes et
287 al., 2020) were analyzed to account for total lymphocyte abundance, age, and sex, people
288 hospitalized with acute respiratory distress syndrome due to COVID-19, had 1.7-fold
289 fewer ILCs (95%CI: 2.38–1.22; p = 0.002) than controls (Supplementary Fig. S2). Also
290 consistent with the main adult cohort studied here, ILC abundance was not significantly
291 reduced in the group of patients with less severe disease (Supplementary Fig. S2).
292

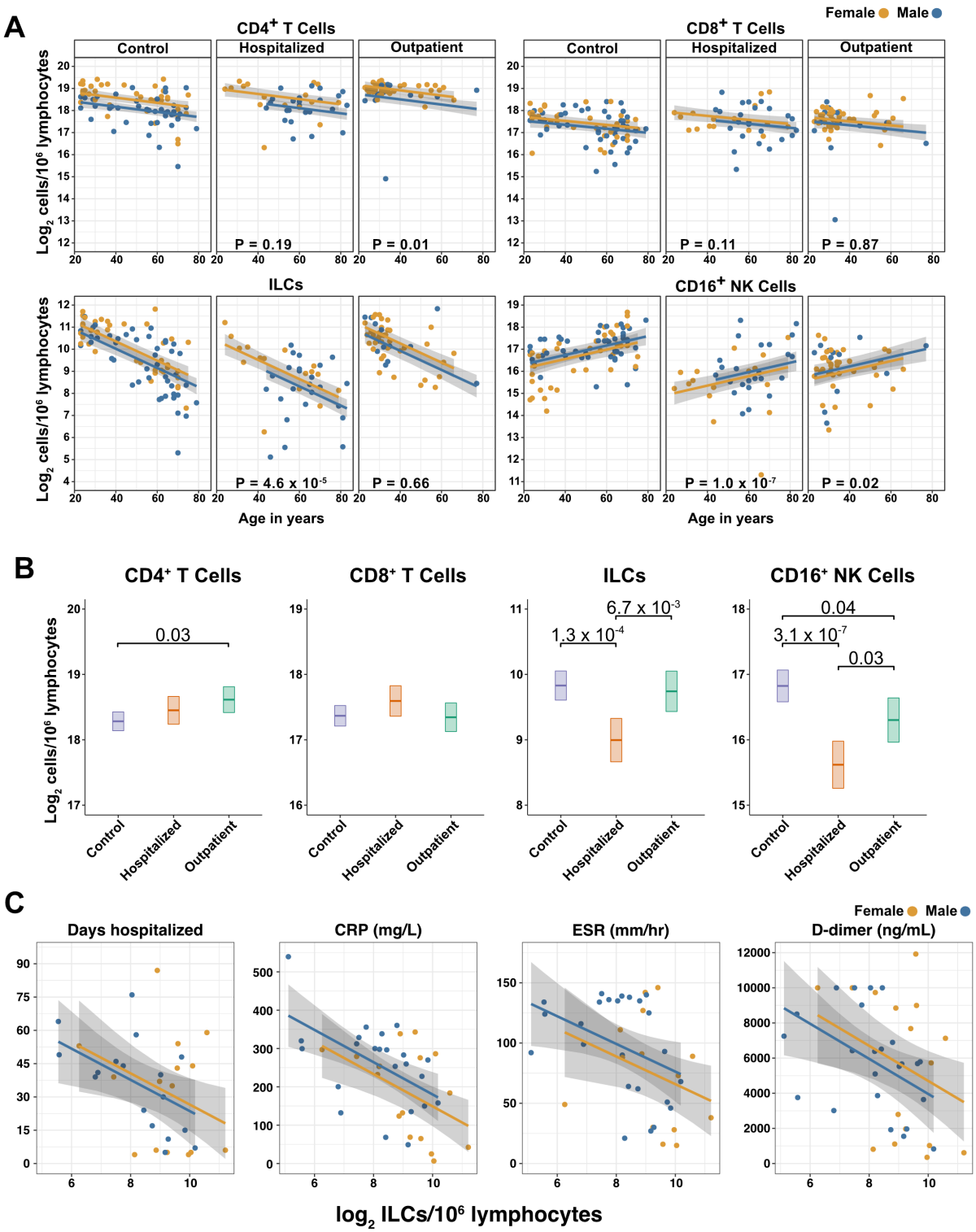

293

294 **Fig. 3. Innate lymphoid cells are depleted in adults hospitalized with COVID-19 and**

295 **ILC abundance correlates inversely with disease severity.**

296 (**A**) Effect of age (X-axis) on log2 abundance per million total lymphocytes of the indicated
297 lymphoid cell populations (Y-axis), as determined by the regression analysis in Table 2.
298 Each dot represents an individual blood donor, with yellow for female and blue for male.
299 Shading represents the 95%CI. P-values are from the regression analysis for
300 comparisons to the control group.
301 (**B**) Log2 abundance per million lymphocytes of the indicated lymphoid cell populations,
302 shown as estimated marginal means with 95%CI, generated from the multiple linear
303 regressions in Table 2, and averaged across age and sex. P-values represent pairwise
304 comparisons on the estimated marginal means, adjusted for multiple comparisons with
305 the Tukey method. Adjusted P-values < 0.05 are shown.
306 (**C**) Association of the indicated clinical parameters with log2 abundance of ILCs per
307 million lymphoid cells. Regression lines are from simplified multiple regression models to
308 permit visualization on a two-dimensional plane. Shading represents the 95%CI. Results
309 of the full models accounting for effects of both age and sex, are reported in Table 4 and
310 the text.
311
312
313
314
315
316
317
318

319 **Odds of hospitalization in adults infected with SARS-CoV-2 increases with**
320 **decreasing number of ILCs**

321 Multiple logistic regression was used next to determine whether differences in abundance
322 of any lymphoid cell subset was associated with odds of hospitalization in people infected
323 with SARS-CoV-2. The adjusted odds ratio was calculated using lymphoid cell subset
324 abundance, age, sex, and duration of symptoms at the time of blood draw, each as
325 independent variables. Abundance of ILCs, but not of $CD16^+$ NK cells, $CD4^+$ T cells, or
326 $CD8^+$ T cells was associated with odds of hospitalization: the odds ratio for hospitalization,
327 adjusted for age, sex, and symptom duration, was 0.413 (95%CI: 0.197–0.724; p =
328 0.00691), an increase of 58.7% for each 2-fold decrease in ILC abundance (Table 3).

329

Table 3: Odds of Hospitalization[a]

Cell count[b]	Odds Ratio[c]	95% Confidence Interval	P-Value
$CD4^+$ T	0.501	0.184–1.07	0.106
ILC	0.413	0.197–0.724	0.007
$CD8^+$ T	1.22	0.635–2.64	0.579
$CD16^+$ NK	0.814	0.53–1.21	0.309

[a]Adjusted for age, sex, and symptom duration at time of sample collection
[b]per 10^6 lymphocytes
[c]per 2-fold increase in cell population abundance

330 **Duration of hospital stay in adults with COVID-19 increases with decreasing ILC**
331 **abundance**

332 The relationship between lymphoid cell abundance and duration of hospitalization was
333 assessed to determine whether the association between ILC abundance and COVID-19

334 severity extended to clinical outcomes within the hospitalized adults. This relationship
335 was assessed with multiple linear regression, including age, sex, and cell abundance as
336 independent variables. Holding age and sex constant, abundance of ILCs, but not of
337 $CD16^+$ NK cells, $CD4^+$ T cells, or $CD8^+$ T cells, was associated with length of time in the
338 hospital: each two-fold decrease in ILC abundance was associated with a 9.38 day
339 increase in duration of hospital stay (95% CI: 15.76–3.01; p = 0.0054) (Fig. 3C and Table
340 4).

Table 4: Association of cell type abundance with time in hospital and laboratory values[a]

Cell count[b]	Days hospitalized	CRP (mg/L)[c]	ESR (mm/h)[c]	D-dimer (ng/mL)[c]
$CD4^+$ T	-10.843	-3.335	-2.674	-1868.847*
	[-22.511, 0.825]	[-56.162, 49.492]	[-23.840, 18.492]	[-3375.630, -362.063]
ILC	-9.381**	-46.288***	-11.035*	-1098.515*
	[-15.755, -3.008]	[-71.337, -21.238]	[-21.936, -0.134]	[-1932.842, -264.188]
$CD8^+$ T	3.366	32.247	15.317	486.192
	[-8.992, 15.724]	[-16.509, 81.003]	[-4.127, 34.761]	[-1049.836, 2022.221]
$CD16^+$ NK	-4.775	-14.619	-5.159	-404.873
	[-11.251, 1.701]	[-44.011, 14.774]	[-16.809, 6.491]	[-1316.261, 506.516]

* $p < 0.05$, ** $p < 0.01$, *** $p < 0.001$
[a]coefficients are for each two-fold increase in cell population abundance, adjusted for age and sex [±95%CI]
[b]per 10^6 lymphoid cells
[c]Maximum lab value recorded during course of hospitalization

341 **ILC abundance correlates inversely with markers of inflammation in adults**
342 **hospitalized with COVID-19**

343 To further characterize the extent to which lymphoid cell abundance predicted COVID-19

344 severity, multiple regression with age, sex, and cell abundance, as independent variables,
345 was performed on peak blood levels of inflammation markers indicative of COVID-19
346 severity: C-reactive protein (CRP) and erythrocyte sedimentation rate (ESR), and the
347 fibrin degradation product D-dimer (Gallo Marin et al., 2020; Gupta et al., 2021; Luo et
348 al., 2020; Zhang et al., 2020; Zhou et al., 2020). Holding age and sex constant, each two-
349 fold decrease in ILC, but not in $CD16^+$ NK cell, $CD4^+$ T cell, or $CD8^+$ T cell abundance,
350 was associated with a 46.29 mg/L increase in blood CRP (95% CI: 71.34–21.24; $p = 6.25$
351 $\times 10^{-4}$) and 11.04 mm/h increase in ESR (95% CI: 21.94–0.13; $p = 0.047$) (Fig. 3C and
352 Table 4). Abundance of both ILCs and $CD4^+$ T cells was associated with blood levels of
353 D-dimer, with each two-fold decrease in cell abundance associated with an increase in
354 D-dimer by 1098.52 ng/mL (95% CI: 1932.84–264.19; $p = 0.011$) and 1868.85 ng/mL
355 (95% CI: 3375.63–362.06; $p = 0.016$), respectively (Table 4).

356 **ILCs are depleted in children and young adults with COVID-19 or MIS-C**

357 Given the decline in ILC abundance with age (Fig.s 2A and 3A, and Table 2), and the
358 inverse relationship between ILC abundance and disease severity in adults (Fig. 3C,
359 Table 3, and Table 4), it was hypothesized that children as a group have less severe
360 COVID-19 because ILC abundance is higher at younger ages, and that pediatric cases
361 with symptomatic SARS-CoV-2 infection, or with MIS-C, are accompanied by significantly
362 lower numbers of ILCs. To test these hypotheses, the abundance of lymphoid cell subsets
363 in pediatric COVID-19 or MIS-C was compared with that from pediatric controls, using
364 multiple linear regression with age, sex, and group as independent variables. Consistent
365 with the findings in adults, blood ILCs in the pediatric cohort decreased with age (Table 5
366 and Fig. 4A), demonstrating that the decrease in ILC abundance across the lifespan is

367 already evident within the first two decades of life. In contrast, significant change over this
368 age range was not detected in the abundance of $CD4^+$ T cells, $CD8^+$ T cells, or $CD16^+$
369 NK cells (Table 5 and Fig 4A).

370 Among pediatric patients with COVID-19, no difference in abundance of the
371 lymphoid cell subsets was associated with hospitalization (Supplementary Table S5), so
372 all pediatric patients treated for COVID-19 were analyzed as a single group. After
373 accounting for effects of age and sex, pediatric patients with COVID-19 had 1.69-fold
374 fewer ILCs (95%CI: 2.73–1.04; p = 0.034) than controls (Fig 4A and Table 5). Neither
375 $CD4^+$ T cells, $CD8^+$ T cells, nor $CD16^+$ NK cells were depleted in pediatric COVID-19
376 patients (Fig 4A and Table 5).

377 As with pediatric COVID-19, ILCs were also lower in MIS-C, with 2.14-fold fewer
378 ILCs (95%CI: 3.69–1.24; p = 0.007) than controls (Fig. 4A and Table 5). However, unlike
379 pediatric COVID-19, individuals with MIS-C had reduced numbers of T cells as compared
380 with pediatric controls, with 1.6-fold fewer $CD4^+$ T cells (95%CI: 2.04–1.26; $p = 3.28 \times 10^{-}$
381 ^{4}) and 1.42-fold fewer $CD8^+$ T cells (95%CI: 1.87–1.07; p = 0.016) (Fig. 4A and Table 5).
382 Depletion of T cells, then, distinguished MIS-C from both pediatric and adult COVID-19.
383 Additionally, consistent with the finding in adults hospitalized with COVID-19 (Fig. 3C and
384 Table 4), after accounting for effect of group, each two-fold decrease in ILC abundance
385 in pediatric patients hospitalized with COVID-19 or MIS-C was associated with a 40.5
386 mg/L increase in blood CRP (95% CI: 77.87–3.13; p = 0.035) (Fig. 4C), and no such
387 association was detected with $CD4^+$ T cells, $CD8^+$ T cells, or CD16+ NK cells.

388

389

Table 5: Change in Pediatric Cohort Cell Abundance Due to Age, Sex, and Group

Fold difference (log2) [±95%CI]				
	CD4⁺ T[a]	**ILC[a]**	**CD8⁺ T[a]**	**CD16⁺ NK[a]**
Age	-0.004	-0.083**	0.012	0.004
	[-0.027, 0.019]	[-0.135, -0.032]	[-0.014, 0.039]	[-0.060, 0.068]
Male	-0.219	-0.027	0.060	-0.343
	[-0.492, 0.054]	[-0.640, 0.586]	[-0.249, 0.370]	[-1.098, 0.413]
COVID	0.018	-0.754*	-0.088	0.416
	[-0.290, 0.327]	[-1.447, -0.061]	[-0.432, 0.257]	[-0.424, 1.257]
MIS-C	-0.678***	-1.098**	-0.503*	-0.498
	[-1.028, -0.328]	[-1.884, -0.313]	[-0.904, -0.101]	[-1.479, 0.483]
R^2	0.359	0.342	0.169	0.106

* $p < 0.05$, ** $p < 0.01$, *** $p < 0.001$
[a]per 10^6 lymphocytes

The above analysis of lymphoid cell subsets in pediatric COVID-19 and MIS-C was performed in comparison to pediatric controls alone. Results were essentially unchanged when multiple linear regression was repeated with combined pediatric and adult control groups (Fig. 4B, Supplementary Fig. S3, and Supplementary Table S6).

Pediatric MIS-C is distinguished from COVID-19 by recovery of ILCs during follow-up

The availability of follow-up samples in this pediatric cohort provided the opportunity to assess the abundance of lymphoid subsets after recovery from illness. To this end, a linear mixed model was fit to determine the change in ILC abundance from acute illness

400 to follow-up in 10 individuals (5 COVID-19 and 5 MIS-C) for whom both acute and follow-
401 up samples were available. After accounting for effects of age, sex, and group, individuals
402 recovering from MIS-C had a 2.39-fold increase in ILC abundance (95%CI: 1.49–3.81; p
403 = $6.6x10^{-3}$) but there was no significant change in ILC abundance for individuals
404 recovering from COVID-19 (Fig. 4D). Both $CD4^+$ and $CD8^+$ T cells, which were depleted
405 in MIS-C but not in COVID-19, also increased during recovery from MIS-C and remained
406 unchanged during recovery from COVID-19 (Supplementary Fig. S4).

407 The relationship between time to follow-up and lymphoid cell abundance was then
408 examined for all available follow-up samples whether or not a paired sample from the
409 acute illness was available (COVID-19, N=14; MIS-C, N=7). This analysis found no
410 relationship between time to follow-up and abundance of any lymphoid subset, and that
411 individuals recovering from MIS-C had 2.28-fold more ILCs (95%CI: 1.11–4.69; p =
412 0.0265) than individuals recovering from COVID-19 (Fig. 4E). There was no difference
413 between the follow-up groups in $CD4^+$ T cells, $CD8^+$ T cells, or $CD16^+$ NK cells (Fig. 4E).
414 Interestingly, prior to being hospitalized with MIS-C, only one of these patients had
415 COVID-19 symptoms and, despite low ILC abundance in the COVID-19 follow-up cohort,
416 only 28.6% of this group had been ill enough to require hospitalization (Supplementary
417 Table S2).

418 Differences between COVID-19 and MIS-C in regards to T cell depletion and ILC
419 recovery during follow-up indicate that the underlying processes causing lower ILC
420 abundance in these two SARS-CoV-2-associated diseases are different.

421

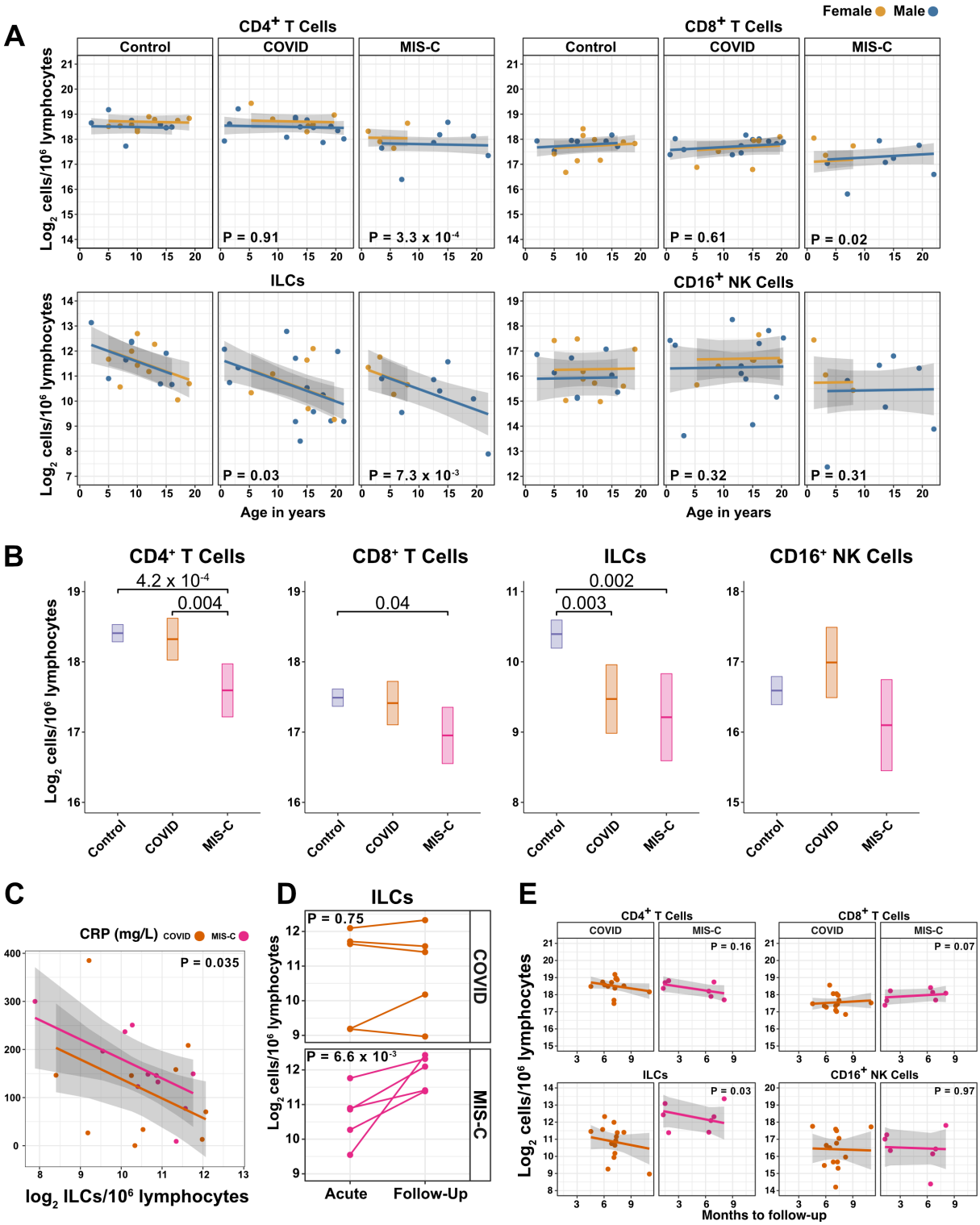

Fig. 4. ILCs are depleted in children with COVID-19 or MIS-C

424 (**A**) Effect of age (X-axis) on log2 abundance per million lymphocytes of the indicated
425 lymphoid cell populations (Y-axis), as determined by the regression analysis in Table 5.
426 Each dot represents an individual blood donor, with yellow for female and blue for male.
427 Shading represents the 95%CI. P-values are from the regression analysis for
428 comparisons to the control group.
429 (**B**) Log2 abundance per million lymphocytes of the indicated lymphoid cell populations,
430 shown as estimated marginal means with 95%CI, generated from the multiple linear
431 regressions in Table S6 that included the combined pediatric and adult control data, and
432 averaged across age and sex. P-values represent pairwise comparisons on the estimated
433 marginal means, adjusted for multiple comparisons with the Tukey method. Adjusted P-
434 values < 0.05 are shown.
435 (**C**) Association of CRP with log2 abundance of ILCs per million lymphocytes. Shading
436 represents the 95%CI. Each dot represents a single blood donor, orange for COVID-19,
437 magenta for MIS-C. P-value is for the effect of ILC abundance on CRP as determined by
438 linear regression.
439 (**D**) Log2 ILC abundance per million lymphocytes in longitudinal pairs of samples
440 collected during acute presentation and during follow-up, from individual children with
441 COVID-19 or MIS-C. Each pair of dots connected by a line represents an individual blood
442 donor. P-values are for change in ILC abundance at follow-up, as determined with a linear
443 mixed model, adjusting for age, sex, and group, and with patient as a random effect.
444 (**E**) Effect of time to follow-up (X-axis) on log2 abundance per million lymphocytes of the
445 indicated lymphoid cell populations (Y-axis). P-values are for the difference between the

446 COVID-19 and MIS-C follow-up groups, independent of time to follow-up as determined
447 by linear regression. Shading represents the 95%CI.

448 **Blood ILCs resemble homeostatic ILCs isolated from lung**

449 In response to the observations described above regarding abundance of blood ILCs and
450 severity of COVID-19 attempts were made to extend these studies to lung ILCs. It was
451 not possible to obtain lung samples from people with COVID-19. However, ILCs circulate
452 from tissues to the bloodstream in lymphatic drainage via the thoracic duct suggesting
453 that measurement of blood ILCs could provide a surrogate for assessment of tissue-
454 resident ILCs, including those from the lung. Furthermore, reduction in blood ILCs in
455 people living with HIV-1 infection is paralleled by decreased ILC numbers within the
456 lamina propria of the colon (Wang et al., 2020), and so the lower abundance of blood
457 ILCs associated with severe COVID-19 might be paralleled by decreased abundance of
458 homeostatic ILCs in the lung.

459 Given the inability to assess lung samples from people with COVID-19, RNA
460 sequencing (RNA-Seq) was performed on blood ILCs from nine healthy controls and
461 these data were compared to previously published RNA-Seq profiles of ILCs sorted from
462 lung, spleen, and intestine (Ardain et al., 2019; Yudanin et al., 2019). Unbiased principal
463 component analysis demonstrated overlap of blood ILCs with lung ILCs and clear
464 separation from ILCs of jejunum or spleen (Fig. 5A). 355 genes were consistently
465 differentially expressed (fold-change > 1.5, padj < 0.01) when either blood or lung ILCs
466 were compared to ILCs from the other tissues (Fig. 5B,C). Gene ontology analysis
467 demonstrated enrichment for terms associated with type 2 immunity (Supplementary
468 Table S7). Genes significantly higher in both blood and lung ILCs included the ILC2-

469 defining genes GATA3 and PTGDR2 (CRTH2), as well as other genes important for ILC
470 development such as TCF7 (Yang et al., 2013) (Fig. 5B,C). As confirmation of the RNA
471 signature, TCF7- and CRTH2-encoded proteins were detected in blood ILCs by flow
472 cytometry (Fig. 6A).

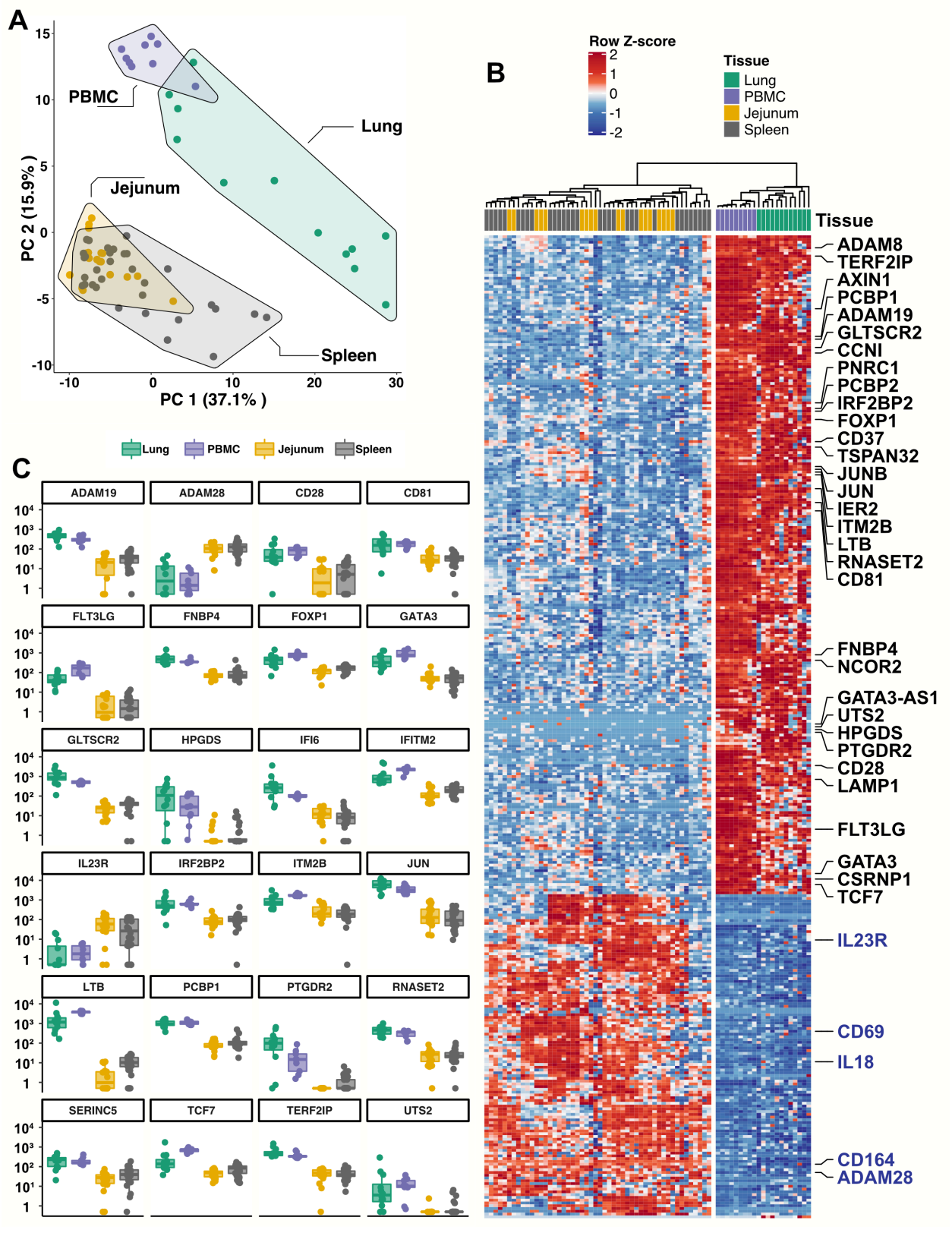

Fig. 5. Blood ILCs are transcriptionally similar to lung ILCs

475 RNA-seq of ILCs sorted from blood of 9 SARS-CoV-2-uninfected controls in comparison
476 to RNA-seq data of ILCs sorted from jejunum, lung, and spleen.
477 (**A**) PCA plot of first two principal components calculated from the top 250 most variable
478 genes across all samples. Each dot represents an individual sample with blue for ILCs
479 sorted from blood, green for lung, yellow for jejunum, and grey for spleen.
480 (**B**) Heatmap of 355 genes differentially expressed (fold-change > 1.5, padj < 0.01 as
481 determined with DESeq2) between either blood or lung ILCs and ILCs from the other
482 tissues.
483 (**C**) Select genes from (B) plotted as deseq2 normalized counts. Each dot represents an
484 individual sample with blue for ILCs sorted from blood, green for lung, yellow for jejunum,
485 and grey for spleen. Boxplots represent the distribution of the data with the center line
486 drawn through the median with the upper and lower bounds of the box at the 75th and
487 25th percentiles respectively. The upper and lower whiskers extend to the largest or
488 smallest values within 1.5 x the interquartile range (IQR).
489
490
491
492
493
494
495
496

497 **Blood ILCs are functional ILC2s capable of producing AREG**

498 To assess the function of blood ILCs, PBMCs were stimulated with PMA and ionomycin,
499 and assayed by flow cytometry for production of IL-13 after intracellular cytokine staining
500 and gating on ILCs. IL-13 was detected in the stimulated ILC population (Fig. 6B),
501 demonstrating that the majority of blood ILCs function as ILC2s. Additionally, the blood
502 ILCs produced amphiregulin (Fig. 6B), a protein implicated in the promotion of disease
503 tolerance by ILCs in animal models (Branzk et al., 2018; Diefenbach et al., 2020;
504 Jamieson et al., 2013; McCarville and Ayres, 2018; Monticelli et al., 2015, 2011).

505 **Females have a higher fraction of amphiregulin-producing blood ILCs than do**
506 **males**

507 Given the role AREG-producing ILCs play in maintaining disease tolerance in animal
508 models (Branzk et al., 2018; Diefenbach et al., 2020; McCarville and Ayres, 2018;
509 Monticelli et al., 2015, 2011), sex differences in the functional capability of these ILCs
510 could contribute to the greater risk for severe COVID-19 in males (O'Driscoll et al.,
511 2020). To address this hypothesis, ILCs isolated from peripheral blood of controls were
512 stimulated with PMA and ionomycin, and assayed by flow cytometry for AREG
513 production. Consistent with the apparently lower disease tolerance in males, males had
514 a lower median fraction of $AREG^+$ ILCs than did females (P=0.018) (Fig. 6C). This
515 difference was also reflected in a significantly lower AREG Mean Fluorescent Intensity
516 (MFI) in males, and neither fraction of $AREG^+$ ILCs nor AREG MFI was affected by age
517 (Supplementary Fig. S5).

518

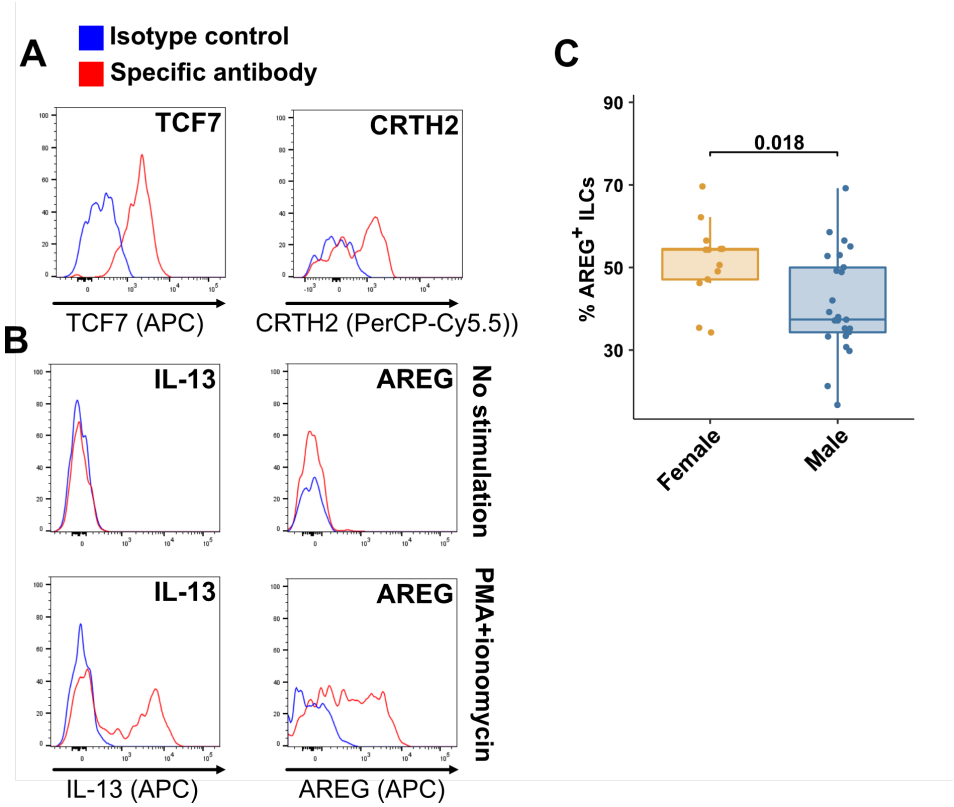

Fig. 6. Peripheral blood ILCs exhibit homeostatic ILC2 functions

(**A-B**) Flow cytometry for the indicated proteins. Cells in (A) were assayed at steady-state and cells in (B) were assayed either at steady-state or after stimulation with PMA and ionomycin, as indicated. Detection of surface proteins was performed on ILCs gated as $Lin^{-}CD56^{-}CD127^{+}$ and detection of intracellular proteins was performed on ILCs gated as $Lin^{-}TBX21^{-}CD127^{+}$.

(**C**) Percent of $AREG^{+}$ ILCs in blood of control blood donors after stimulation with PMA and ionomycin. Each dot represents an individual blood donor. Boxplots represent the distribution of the data with the center line drawn through the median with the upper and lower bounds of the box at the 75th and 25th percentiles respectively. The upper and lower whiskers extend to the largest or smallest values within 1.5 x the interquartile range (IQR). P-value is from a two-sided, Wilcoxon rank-sum test.

532 # DISCUSSION

533 The outcome of SARS-CoV-2 infection ranges from entirely asymptomatic to lethal
534 COVID-19 (Cevik et al., 2021; He et al., 2021; Jones et al., 2021; Lee et al., 2020; Lennon
535 et al., 2020; Ra et al., 2021; Richardson et al., 2020; Yang et al., 2021). Yet, viral load
536 does not reliably discriminate asymptomatic from symptomatic or hospitalized
537 populations (Cevik et al., 2021; Jones et al., 2021; Lee et al., 2020; Lennon et al., 2020;
538 Ra et al., 2021; Yang et al., 2021). In contrast, demographic factors, including increasing
539 age and male sex, predict worse outcome of SARS-CoV-2 infection (Alkhouli et al., 2020;
540 Bunders and Altfeld, 2020; Gupta et al., 2021; Laxminarayan et al., 2020; Mauvais-Jarvis,
541 2020; O'Driscoll et al., 2020; Peckham et al., 2020; Richardson et al., 2020; Scully et al.,
542 2020). These demographic risk factors could be due to sexual dimorphism and changes
543 with aging in composition and function of the human immune system (Darboe et al., 2020;
544 Klein and Flanagan, 2016; Márquez et al., 2020; Patin et al., 2018; Solana et al., 2012).
545 Therefore it is necessary to account for effects of age and sex to determine if there are
546 additional, independent, effects of SARS-CoV-2-associated disease.

547 This study collected and analyzed 245 blood samples from 177 adult and 58
548 pediatric patients and controls, spanning the ages of 0.7 to 83 years, with approximately
549 equal numbers of males and females. It was therefore possible to characterize the
550 independent effects of age, sex, COVID-19, and MIS-C on blood lymphoid cell
551 populations. After accounting for effects of age and sex, ILCs, but not $CD4^+$ or $CD8^+$ T
552 cells, were lower in individuals hospitalized with COVID-19 when compared with controls
553 (Table 2 and Fig. 3A,B). Lower numbers of ILCs were also observed in children with
554 COVID-19 (Table 5 and Fig. 4A,B), as well as in an independent cohort of adult patients

555 (Supplementary Fig. S2). Among adults infected with SARS-CoV-2, lower abundance of
556 ILCs, but not of the other lymphoid cell subsets, was associated with increased odds of
557 hospitalization, longer duration of hospitalization, and higher blood level of factors
558 associated with systemic inflammation, including CRP (Tables 3 and 4, and Fig. 3C). This
559 inverse relationship between ILC abundance and CRP was also evident in children with
560 COVID-19 or MIS-C (Fig. 4C).

561 The identification of reduced ILC numbers as uniquely related to COVID-19
562 severity is important as these cells mediate disease tolerance in animal models (Artis and
563 Spits, 2015; Branzk et al., 2018; Califano et al., 2018; Diefenbach et al., 2020; McCarville
564 and Ayres, 2018; Monticelli et al., 2015, 2011). The results here therefore indicate that
565 loss of ILCs from blood correlates with loss of ILC-associated homeostatic functions,
566 thereby allowing more severe COVID-19. Although this study examined circulating blood
567 lymphoid cells, and does not provide direct information about processes occurring within
568 tissues, transcriptional and functional characterization of blood ILCs demonstrated that
569 these cells are similar to ILCs isolated from lung tissue (Fig. 5). Human ILCs circulate in
570 lymphatic fluid draining from the tissues to the blood via the thoracic duct, raising the
571 possibility that some ILCs in the blood originate from, or traffic to, lung tissue. Further
572 characterization of these blood ILCs showed that they are functional ILC2s capable of
573 producing the protein AREG (Fig. 6A,B). Given the tissue homeostatic role AREG plays
574 in animal models of disease tolerance (Branzk et al., 2018; Diefenbach et al., 2020;
575 Jamieson et al., 2013; McCarville and Ayres, 2018; Monticelli et al., 2015, 2011), the
576 discovery here that males have a smaller fraction than females of blood ILCs capable of
577 producing AREG (Fig. 6C) could explain why males are at greater risk of death from

578 SARS-CoV-2 infection (O'Driscoll et al., 2020). This sexual dimorphism in ILC function
579 would be amplified further by the lower overall abundance of ILCs in males (Fig. 2B and
580 Table 3).

581 Although the inverse relationship between the number of blood ILCs and severity
582 of COVID-19 suggests that loss of ILC homeostatic function results in breakdown of
583 disease tolerance (Arpaia et al., 2015; Artis and Spits, 2015; Branzk et al., 2018;
584 Diefenbach et al., 2020; McCarville and Ayres, 2018; Monticelli et al., 2015, 2011), this
585 observational study cannot determine whether ILC depletion preceded SARS-CoV-2
586 infection or whether ILC numbers are depleted as a consequence of SARS-CoV-2
587 infection. However, several observations support the hypothesis that individuals with
588 lower ILC numbers at the time of SARS-CoV-2 infection are at greater risk of developing
589 severe disease. ILC numbers in uninfected controls decrease exponentially with age; this
590 decrease is much larger than that seen with other lymphoid cell types (Fig. 2A), and much
591 more closely mirrors the exponential increase in COVID-19 mortality with age (O'Driscoll
592 et al., 2020) (Fig. 2C). In addition, the greater risk of COVID-19 mortality in males
593 (O'Driscoll et al., 2020) correlates with lower abundance of blood ILCs (Fig. 2B and Table
594 3) and smaller fraction of ILCs capable of producing AREG (Fig. 6C). Further supporting
595 this hypothesis is the observation that conditions independently associated with lower ILC
596 abundance, such as HIV-1 infection (Kløverpris et al., 2016; Wang et al., 2020) and
597 obesity (Brestoff et al., 2015; Yudanin et al., 2019), increase the risk for worse outcomes
598 from SARS-CoV-2 infection (Biccard et al., 2021; Kompaniyets, 2021; Tesoriero et al.,
599 2021).

600 In contrast to individuals with COVID-19, children with MIS-C had lower numbers

601 of T cells as well as ILCs (Table 5 and Fig. 4A,B), and longitudinal follow-up samples for
602 pediatric COVID-19 and MIS-C patients showed persistence of low ILC numbers after
603 COVID-19, but normalization of all depleted cell types after recovery from MIS-C (Fig.
604 4D,E and Supplementary Fig. S4). These differences imply that the reversible
605 lymphopenia in MIS-C is due to different underlying processes than the more specific and
606 persistent lower ILC abundance seen in individuals with COVID-19. This difference is
607 made more interesting by the fact that none of the children with MIS-C had required
608 hospitalization for COVID-19 and only one experienced any COVID-19 symptoms. The
609 other children with MIS-C were therefore unaware that they had been infected. It is
610 possible that children with pre-existing lower ILC numbers are at risk of developing
611 COVID-19 if infected with SARS-CoV-2, while other factors such as prolonged exposure
612 to SARS-CoV-2 antigens in the gastrointestinal tract (Yonker et al., 2021), or rare inborn
613 errors of immunity (Sancho-Shimizu et al., 2021), promote inflammatory processes in
614 MIS-C that drive nonspecific lymphoid cell depletion, which ultimately normalizes after
615 recovery.

616 Although ILC depletion and recovery has been reported in rheumatoid arthritis
617 (Rauber et al., 2017), inflammation-driven ILC-depletion is not necessarily reversible, as
618 ILCs appear permanently depleted after HIV-1 infection, possibly by high levels of
619 common γ-chain cytokines during acute infection (Wang et al., 2020). Better
620 understanding of the processes that drive down ILC abundance in populations
621 susceptible to COVID-19 could potentially allow for development of interventions that
622 increase ILC abundance and restore homeostatic disease tolerance mechanisms.

623 In conclusion, considering the established homeostatic function of ILCs (Artis and

624 Spits, 2015; Branzk et al., 2018; Klose and Artis, 2016; Monticelli et al., 2015, 2011) and
625 presumed non-immunologic, host adaptive responses necessary to survive pathogenic
626 infection (López-Otín and Kroemer, 2021; McCarville and Ayres, 2018; Medzhitov et al.,
627 2012; Schneider and Ayres, 2008), the findings reported here support the hypothesis that
628 loss of disease tolerance mechanisms attributable to ILCs increase the risk of morbidity
629 and mortality with SARS-CoV-2 infection. The findings of this observational study warrant
630 establishment of prospective cohorts to determine whether abundance of ILCs or of other
631 lymphoid cell subsets associated with disease tolerance (Arpaia et al., 2015; Artis and
632 Spits, 2015; Branzk et al., 2018; Diefenbach et al., 2020; McCarville and Ayres, 2018;
633 Monticelli et al., 2015, 2011), predict clinical outcome for infection with SARS-CoV-2 or
634 other lethal pathogens. Understanding the mechanisms that allow an individual to tolerate
635 high-level viral replication without experiencing symptoms, and how these mechanisms
636 can fail and thereby allow for progression to severe disease, will provide the foundation
637 for development of therapeutic interventions that maintain health and improve survival of
638 pathogenic viral infection (Ayres, 2020b).
639
640
641
642
643
644
645
646
647

648 ## Materials and Methods

649 ### Data availability

650 The data that support the findings of this study are available within the manuscript and in
651 its supplementary information files. Bulk RNA-seq datasets generated here can be found
652 at: NCBI Gene Expression Omnibus (GEO): GSE168212. Bulk RNA-seq data generated
653 by previously-published studies are available from NCBI GEO: GSE131031 and
654 GSE126107. This study did not generate unique code. Any additional information
655 required to reanalyze the data reported in this paper is available from the lead contact
656 upon request.

657 ### Peripheral blood PBMCs

658 As part of a COVID-19 observational study, peripheral blood samples were collected from
659 91 adults with SARS-CoV-2 infection at the Massachusetts General Hospital and affiliated
660 outpatient clinics. Request for access to coded patient samples was reviewed by the
661 Massachusetts Consortium for Pathogen Readiness (https://masscpr.hms.harvard.edu/),
662 and approved by the University of Massachusetts Medical School IRB (protocol
663 #H00020836). Pediatric participants with COVID-19 or MIS-C were enrolled in the
664 Massachusetts General Hospital Pediatric COVID-19 Biorepository (MGB IRB #
665 2020P000955); healthy pediatric controls were enrolled in the Pediatric Biorepository
666 (MGB IRB # 2016P000949). Samples were collected after obtaining consent from the
667 patient if 18 years or older, or from the parent/guardian, plus assent when appropriate.
668 Demographic, laboratory, and clinical outcome data were included with the coded
669 samples. Samples from 86 adult blood donors and 17 pediatric blood donors, either

670 collected prior to the SARS-CoV-2 outbreak, or from healthy individuals screened at a
671 blood bank, were included as controls.
672
673 **Human mononuclear cell isolation**
674 Human peripheral blood was diluted in an equal volume of RPMI-1640 (Gibco), overlaid
675 on Lymphoprep (STEMSELL, 07851), and centrifuged at 500 x g at room temperature for
676 30 minutes. Mononuclear cells were washed 3 times with MACS buffer (0.5% BSA and 2
677 mM EDTA in PBS) and frozen in FBS containing 10% DMSO.
678
679
680 **Flow cytometry**
681 Peripheral blood mononuclear cells (PBMCs) were first stained with Live and Dead violet
682 viability kit (Invitrogen, L-34963). To detect surface molecules, cells were stained in
683 MACS buffer with antibodies (Supplementary Table S8) for 30 min at 4°C in the dark. To
684 detect IL-13 or AREG, cells were stimulated with PMA and ionomycin (eBioscience, 00-
685 4970-03) for 3 hours with Brefeldin A and Monensin (eBioscience, 00-4980-03) present
686 during the stimulation. To detect transcription factors or cytokines, cells were fixed and
687 permeabilized using Foxp3 staining buffer kit (eBioscience, 00-5523-00), then
688 intracellular molecules were stained in permeabilization buffer with antibodies. Cells were
689 detected on a BD Celesta flow cytometer using previously established gating strategies
690 (Wang et al., 2020). Cell subsets were identified using FlowJo™ software (Becton,
691 Dickson and Company). Representative gating strategies are shown in Fig. S6.

692 **Bulk RNA-Seq Library preparation of PBMC ILCs**

693 The sequencing libraries were prepared using CEL-Seq2 (Hashimshony et al., 2016).
694 RNA from sorted cells was extracted using TRIzol reagent (ThermoFisher, 15596018).
695 10 ng RNA was used for first strand cDNA synthesis using barcoded primers (the specific
696 primers for each sample were listed in Supplementary Table S9). The second strand was
697 synthesized by NEBNext Second Strand Synthesis Module (NEB, E6111L). The pooled
698 dsDNA was purified with AMPure XP beads (Beckman Coulter, A63880), and subjected
699 to in vitro transcription (IVT) using HiScribe T7 High Yield RNA Synthesis Kit (NEB,
700 E2040S), then treated with ExoSAP-IT (Affymetrix, 78200). IVT RNA was fragmented
701 using RNA fragmentation reagents (Ambion), and underwent another reverse
702 transcription step using random hexamer RT primer-5'-GCC TTG GCA CCC GAG AAT
703 TCC ANN NNN N-3' to incorporate the second adapter. The final library was amplified
704 with indexed primers: RP1 and RPI1 (Supplementary Table S9), and the bead purified
705 library was quantified with 4200 TapeStation (Agilent Technologies), and paired-end
706 sequenced on Nextseq 500 V2 (Illumina), Read 1: 15 cycles; index 1: 6 cycles; Read 2:
707 60 cycles.

708

709 **RNA-seq analyses**

710 Pooled reads from PBMC ILCs were separated by CEL-Seq2 barcodes, and
711 demultiplexed reads from RNA-seq of ILCs from lung (Ardain et al., 2019), spleen and
712 intestine (Yudanin et al., 2019), were downloaded from GSE131031 and GSE126107.
713 Within the DolphinNext RNA-seq pipeline (Revision 4) (Yukselen et al., 2020), reads were
714 aligned to the hg19 genome using STAR (version 2.1.6) (Dobin et al., 2013) and counts

715 of reads aligned to RefSeq genes were quantified using RSEM (version 1.3.1) (Li and
716 Dewey, 2011). Normalized transcript abundance in the form of TPMs were used to filter
717 out low abundance transcripts with an average of <3 TPMs across libraries. RSEM-
718 generated expected counts were normalized and differential analysis was performed
719 using DEseq2 (Love et al., 2014) in R, with significant genes defined as a greater than
720 1.5-fold difference and an adjusted p-value <0.01. GO Enrichment Analysis was
721 performed in R using the enrichGO function in the clusterProfiler R package (Yu et al.,
722 2012). Data were transformed using vsd within DEseq2 both for the heatmap visualization
723 with ComplexHeatmap (Gu et al., 2016) and for principal component analysis (PCA) with
724 prcomp on the top 250 most variable genes. Normalized counts were generated for
725 plotting using the counts command in Deseq2.
726
727 **Statistical analysis and data visualization**
728 Data were prepared for analysis with tidyverse packages (Wickham et al., 2019) and
729 visualized using the ggplot2 (Wickham, 2016), ggpubr (Kassambara, 2020), and
730 ComplexHeatmap (Gu et al., 2016) packages, within the R computer software
731 environment (version 4.0.2) (R Core Team, 2020). Group differences were determined
732 with pairwise, two-sided, Wilcoxon rank-sum tests, or Fisher's exact test, as indicated,
733 with Bonferroni correction for multiple comparisons. Multiple linear regression analyses
734 were performed with dependent and independent variables as indicated in the text, using
735 the lm function in R. Pairwise group comparisons on estimated marginal means
736 generated from multiple linear regression were performed using the emmeans package
737 (Lenth, 2020) in R, with multiple comparison correction using the Tukey adjustment.
738 Multiple logistic regressions were performed using the glm function in R. Longitudinal

follow-up analyses on pediatric COVID-19 and MIS-C was performed with linear mixed-effect models using lme4 (Bates et al., 2015) in R with the equation: log2 (lymphoid cell abundance) ~ Age + Sex + Group + Group:Follow_up + (1|Patient_ID). This model tested the effect of followup on ILC abundance in the pediatric COVID-19 and MIS-C groups while accounting for age, sex, and group. Statistical significance was determined with lmerTest (Kuznetsova et al., 2017) in R, using the Satterthwarte's degrees of freedom method. $p<0.05$ was considered significant. United States SARS-CoV-2 infection and mortality data were downloaded from (CDC Case Surveillance Task Force, 2020) and cases with age group and outcome available were plotted by age group as indicated. Mortality rate was calculated by dividing the number of fatal cases by the total number of cases with known outcome in each age group as indicated.

760 **REFERENCES**

761 Alghamdi IG, Hussain II, Almalki SS, Alghamdi MS, Alghamdi MM, El-Sheemy MA. 2014.
762 The pattern of Middle East respiratory syndrome coronavirus in Saudi Arabia: a
763 descriptive epidemiological analysis of data from the Saudi Ministry of Health. *Int*
764 *J Gen Med* **7**:417.

765 Alkhouli M, Nanjundappa A, Annie F, Bates MC, Bhatt DL. 2020. Sex Differences in Case
766 Fatality Rate of COVID-19: Insights From a Multinational Registry. *Mayo Clin Proc*
767 **95**:1613–1620.

768 Anegon I, Cuturi MC, Trinchieri G, Perussia B. 1988. Interaction of Fc receptor (CD16)
769 ligands induces transcription of interleukin 2 receptor (CD25) and lymphokine
770 genes and expression of their products in human natural killer cells. *J Exp Med*
771 **167**:452–472.

772 Ardain A, Domingo-Gonzalez R, Das S, Kazer SW, Howard NC, Singh A, Ahmed M,
773 Nhamoyebonde S, Rangel-Moreno J, Ogongo P, Lu L, Ramsuran D, de la Luz
774 Garcia-Hernandez M, K. Ulland T, Darby M, Park E, Karim F, Melocchi L,
775 Madansein R, Dullabh KJ, Dunlap M, Marin-Agudelo N, Ebihara T, Ndung'u T,
776 Kaushal D, Pym AS, Kolls JK, Steyn A, Zúñiga J, Horsnell W, Yokoyama WM,
777 Shalek AK, Kløverpris HN, Colonna M, Leslie A, Khader SA. 2019. Group 3 innate
778 lymphoid cells mediate early protective immunity against tuberculosis. *Nature*
779 **570**:528–532.

780 Arpaia N, Green JA, Moltedo B, Arvey A, Hemmers S, Yuan S, Treuting PM, Rudensky
781 AY. 2015. A Distinct Function of Regulatory T Cells in Tissue Protection. *Cell*
782 **162**:1078–1089.

783 Artis D, Spits H. 2015. The biology of innate lymphoid cells. *Nature* **517**:293–301.

784 Ayres JS. 2020a. The Biology of Physiological Health. *Cell* **181**:250–269.

785 Ayres JS. 2020b. Surviving COVID-19: A disease tolerance perspective. *Sci Adv*
786 **6**:eabc1518.

787 Bates D, Mächler M, Bolker B, Walker S. 2015. Fitting Linear Mixed-Effects Models
788 Usinglme4. *Journal of Statistical Software*. doi:10.18637/jss.v067.i01

789 Biccard BM, Gopalan PD, Miller M, Michell WL, Thomson D, Ademuyiwa A, Aniteye E,
790 Calligaro G, Chaibou MS, Dhufera HT, Elfagieh M, Elfiky M, Elhadi M, Fawzy M,
791 Fredericks D, Gebre M, Bayih AG, Hardy A, Joubert I, Kifle F, Kluyts H-L, Macleod
792 K, Mekonnen Z, Mer M, Morais A, Msosa V, Mulwafu W, Ndonga A, Ngumi Z,
793 Omigbodun A, Owoo C, Paruk F, Piercy JL, Scribante J, Seman Y, Taylor E, van
794 Straaten D, Elfiky M, Fawzy M, Awad A, Hussein H, Shaban M, Elbadawy M,
795 Elmehrath AO, Cordie A, Elganainy M, El-Shazly M, Essam M, Abdelwahab OA,
796 Ali A, Hussein AM, Kamel EZ, Monib FA, Ahmed I, Saad MM, Al-Quossi MA,
797 Rafaat N, Galal I, Labib B, Omran DO, Fawzy M, Elfiky M, Azzam Ahmed, Azab
798 M, Tawheed A, Gamal M, El Kassas M, Azzam Aml, Ahmed N, NasrEldin Y,
799 Abdewahab O, Elganainy M, Elmandouh O, Dhufera HT, MeGebre M, Bayih AG,
800 Kifle F, Mekonnen Z, Seman Y, Addisie A, Eshete A, Kifle F, Desita K, Araya H,
801 Agidew Y, Andabo AD, Tesfaye E, Yesuf EA, Hailemariam G, Mohammed MS,
802 Gebremedhin Y, Taye Y, Mebrate TA, Gemechu TB, Bedane TT, Abera ET,
803 Teshome A, Ernest Aniteye EA, Christian Owoo CO, Doku A, Owoo C, Afriyie-
804 Mensah JS, Lawson A, Owoo C, DYaw Sottie DA, Addae E, Ernest Ofosu-Appiah
805 EO-A, William Obeng WO, Ndonga A, Ngumi Z, Ndonga A, Mugera A, Bitta C,

806 Elfagieh M, Elhadi M, Huwaysh MA, Yahya MMA, Mohammed AAK, Majeed AAM,
807 Mohammed AEM, Majeed E, Abusalama AA, Altayr E, Abubaker T, Alkaseek AM,
808 Abdulhafith B, Alziyituni Z, Gamra MF, Anaiba MM, Khel S, Abdelkabir M, Abdeewi
809 S, Adam S, Alhadi A, Alsoufi A, Hassan M, Msherghi A, Bouhuwaish AEM, Msosa
810 V, Mulwafu W, Masoo F, Chikumbanje SS, Mabedi D, Morais A, Carlos A, Morais
811 A, Lorenzoni C, Mambo J, Isabel Chissaque I, Mouzinho Saide M, Chaibou MS,
812 Mamane M, Amadou F, Adesoji Ademuyiwa AA, Akinyinka Omigbodun AO,
813 Adeyeye A, Akinmade A, Momohsani Y, Bamigboye J, Orshio D, Isamade ES,
814 Embu H, Nuhu S, Ojiakor S, Nuhu A, Fowotade A, Sanusi A, Osinaike B, Idowu O,
815 Amali AO, Ibrahim S, Adamu AA, Kida I, Otokwala J, Essam M, Alagbe-Briggs O,
816 Ojum S, Fathima Paruk FP, Juan Scribante JS, Mdladla A, Mabotja T, Naidoo R,
817 Matos-Puig R, Ramkillawan A, Smith M, Arnold-Day C, Thomson D, Calligaro G,
818 Joubert I, Jagga J, Piercy J, Michell L, Devenish L, Miller M, Fernandes N, Gopalan
819 D, Pershad S, Grabowski N, Rammego M, Zwane S, Dhlamini ME, Neuhoff M,
820 Fodo T, Usenbo A, Mrara B, Kabambi F, Cloete E, De Caires L, Dickerson R, Louw
821 C, Theron A, Herselman R, Badenhorst J, Moletsane G, Loots H, Paruk F,
822 Chausse J, Neuhoff M, Sebastian M, Grabowski N, Rheeder P, van Hougenhouck-
823 Tulleken W, Snyman C, Adeleke D, Esterhuizen J, de Man L, Mosola M, van der
824 Linde P, Swart R, Maasdorp S, Martins T, Govender V. 2021. Patient care and
825 clinical outcomes for patients with COVID-19 infection admitted to African high-
826 care or intensive care units (ACCCOS): a multicentre, prospective, observational
827 cohort study. *Lancet* **397**:1885–1894.

828 Branzk N, Gronke K, Diefenbach A. 2018. Innate lymphoid cells, mediators of tissue
829 homeostasis, adaptation and disease tolerance. *Immunol Rev* **286**:86–101.
830 Brestoff JR, Kim BS, Saenz SA, Stine RR, Monticelli LA, Sonnenberg GF, Thome JJ,
831 Farber DL, Lutfy K, Seale P, Artis D. 2015. Group 2 innate lymphoid cells promote
832 beiging of white adipose tissue and limit obesity. *Nature* **519**:242–246.
833 Bunders MJ, Altfeld M. 2020. Implications of Sex Differences in Immunity for SARS-CoV-
834 2 Pathogenesis and Design of Therapeutic Interventions. *Immunity* **53**:487–495.
835 Califano D, Furuya Y, Roberts S, Avram D, McKenzie ANJ, Metzger DW. 2018. IFN-γ
836 increases susceptibility to influenza A infection through suppression of group II
837 innate lymphoid cells. *Mucosal Immunol* **11**:209–219.
838 CDC Case Surveillance Task Force. 2020. COVID-19 Case Surveillance Public Use
839 Data.
840 Cevik M, Tate M, Lloyd O, Maraolo AE, Schafers J, Ho A. 2021. SARS-CoV-2, SARS-
841 CoV, and MERS-CoV viral load dynamics, duration of viral shedding, and
842 infectiousness: a systematic review and meta-analysis. *The Lancet Microbe*
843 **2**:e13–e22.
844 Channappanavar R, Fett C, Mack M, Ten Eyck PP, Meyerholz DK, Perlman S. 2017. Sex-
845 Based Differences in Susceptibility to Severe Acute Respiratory Syndrome
846 Coronavirus Infection. *J Immunol* **198**:4046–4053.
847 Charles Bailey L, Razzaghi H, Burrows EK, Timothy Bunnell H, Camacho PEF, Christakis
848 DA, Eckrich D, Kitzmiller M, Lin SM, Magnusen BC, Newland J, Pajor NM, Ranade
849 D, Rao S, Sofela O, Zahner J, Bruno C, Forrest CB. 2020. Assessment of 135 794

850 Pediatric Patients Tested for Severe Acute Respiratory Syndrome Coronavirus 2
851 Across the United States. *JAMA Pediatr*. doi:10.1001/jamapediatrics.2020.5052
852 Chen G, Wu D, Guo W, Cao Y, Huang D, Wang H, Wang T, Zhang Xiaoyun, Chen H, Yu
853 H, Zhang Xiaoping, Zhang M, Wu S, Song J, Chen T, Han M, Li S, Luo X, Zhao J,
854 Ning Q. 2020. Clinical and immunological features of severe and moderate
855 coronavirus disease 2019. *J Clin Invest* **130**:2620–2629.
856 Chen J, Subbarao K. 2007. The Immunobiology of SARS. *Annu Rev Immunol* **25**:443–
857 472.
858 Cherrier DE, Serafini N, Di Santo JP. 2018. Innate Lymphoid Cell Development: A T Cell
859 Perspective. *Immunity* **48**:1091–1103.
860 Cheung EW, Zachariah P, Gorelik M, Boneparth A, Kernie SG, Orange JS, Milner JD.
861 2020. Multisystem Inflammatory Syndrome Related to COVID-19 in Previously
862 Healthy Children and Adolescents in New York City. *JAMA* **324**:294–296.
863 Cumnock K, Gupta AS, Lissner M, Chevee V, Davis NM, Schneider DS. 2018. Host
864 Energy Source Is Important for Disease Tolerance to Malaria. *Curr Biol* **28**:1635-
865 1642.e3.
866 Darboe A, Nielsen CM, Wolf A-S, Wildfire J, Danso E, Sonko B, Bottomley C, Moore SE,
867 Riley EM, Goodier MR. 2020. Age-Related Dynamics of Circulating Innate
868 Lymphoid Cells in an African Population. *Front Immunol* **11**:594107.
869 Diefenbach A, Gnafakis S, Shomrat O. 2020. Innate Lymphoid Cell-Epithelial Cell
870 Modules Sustain Intestinal Homeostasis. *Immunity* **52**:452–463.

871 Dobin A, Davis CA, Schlesinger F, Drenkow J, Zaleski C, Jha S, Batut P, Chaisson M,
872 Gingeras TR. 2013. STAR: ultrafast universal RNA-seq aligner. *Bioinformatics*
873 **29**:15–21.
874 Donnelly CA, Ghani AC, Leung GM, Hedley AJ, Fraser C, Riley S, Abu-Raddad LJ, Ho
875 L-M, Thach T-Q, Chau P, Chan K-P, Lam T-H, Tse L-Y, Tsang T, Liu S-H, Kong
876 JHB, Lau EMC, Ferguson NM, Anderson RM. 2003. Epidemiological determinants
877 of spread of causal agent of severe acute respiratory syndrome in Hong Kong.
878 *Lancet* **361**:1761–1766.
879 D'Souza SS, Shen X, Fung ITH, Ye L, Kuentzel M, Chittur SV, Furuya Y, Siebel CW,
880 Maillard IP, Metzger DW, Yang Q. 2019. Compartmentalized effects of aging on
881 group 2 innate lymphoid cell development and function. *Aging Cell*.
882 doi:10.1111/acel.13019
883 Feldstein LR, Rose EB, Horwitz SM, Collins JP, Newhams MM, Son MBF, Newburger
884 JW, Kleinman LC, Heidemann SM, Martin AA, Singh AR, Li S, Tarquinio KM, Jaggi
885 P, Oster ME, Zackai SP, Gillen J, Ratner AJ, Walsh RF, Fitzgerald JC, Keenaghan
886 MA, Alharash H, Doymaz S, Clouser KN, Giuliano JS Jr, Gupta A, Parker RM,
887 Maddux AB, Havalad V, Ramsingh S, Bukulmez H, Bradford TT, Smith LS,
888 Tenforde MW, Carroll CL, Riggs BJ, Gertz SJ, Daube A, Lansell A, Coronado
889 Munoz A, Hobbs CV, Marohn KL, Halasa NB, Patel MM, Randolph AG,
890 Overcoming COVID-19 Investigators, CDC COVID-19 Response Team. 2020.
891 Multisystem Inflammatory Syndrome in U.S. Children and Adolescents. *N Engl J*
892 *Med* **383**:334–346.

893 Feldstein LR, Tenforde MW, Friedman KG, Newhams M, Rose EB, Dapul H, Soma VL,
894 Maddux AB, Mourani PM, Bowens C, Maamari M, Hall MW, Riggs BJ, Giuliano JS
895 Jr, Singh AR, Li S, Kong M, Schuster JE, McLaughlin GE, Schwartz SP, Walker
896 TC, Loftis LL, Hobbs CV, Halasa NB, Doymaz S, Babbitt CJ, Hume JR, Gertz SJ,
897 Irby K, Clouser KN, Cvijanovich NZ, Bradford TT, Smith LS, Heidemann SM,
898 Zackai SP, Wellnitz K, Nofziger RA, Horwitz SM, Carroll RW, Rowan CM,
899 Tarquinio KM, Mack EH, Fitzgerald JC, Coates BM, Jackson AM, Young CC, Son
900 MBF, Patel MM, Newburger JW, Randolph AG, Overcoming COVID-19
901 Investigators. 2021. Characteristics and Outcomes of US Children and
902 Adolescents With Multisystem Inflammatory Syndrome in Children (MIS-C)
903 Compared With Severe Acute COVID-19. *JAMA*. doi:10.1001/jama.2021.2091
904 Flanagan KL, Fink AL, Plebanski M, Klein SL. 2017. Sex and Gender Differences in the
905 Outcomes of Vaccination over the Life Course. *Annu Rev Cell Dev Biol* **33**:577–
906 599.
907 Gallo Marin B, Aghagoli G, Lavine K, Yang L, Siff EJ, Chiang SS, Salazar-Mather TP,
908 Dumenco L, Savaria MC, Aung SN, Flanigan T, Michelow IC. 2020. Predictors of
909 COVID-19 severity: A literature review. *Rev Med Virol* e2146.
910 García M, Kokkinou E, Carrasco García A, Parrot T, Palma Medina LM, Maleki KT, Christ
911 W, Varnaitė R, Filipovic I, Ljunggren H-G, Others. 2020. Innate lymphoid cell
912 composition associates with COVID-19 disease severity. *Clinical & translational*
913 *immunology* **9**:e1224.

914 Giefing-Kröll C, Berger P, Lepperdinger G, Grubeck-Loebenstein B. 2015. How sex and
915 age affect immune responses, susceptibility to infections, and response to
916 vaccination. *Aging Cell* **14**:309–321.
917 Gu Z, Eils R, Schlesner M. 2016. Complex heatmaps reveal patterns and correlations in
918 multidimensional genomic data. *Bioinformatics* **32**:2847–2849.
919 Gupta RK, Harrison EM, Ho A, Docherty AB, Knight SR, van Smeden M, Abubakar I,
920 Lipman M, Quartagno M, Pius R, Buchan I, Carson G, Drake TM, Dunning J,
921 Fairfield CJ, Gamble C, Green CA, Halpin S, Hardwick HE, Holden KA, Horby PW,
922 Jackson C, Mclean KA, Merson L, Nguyen-Van-Tam JS, Norman L, Olliaro PL,
923 Pritchard MG, Russell CD, Scott-Brown J, Shaw CA, Sheikh A, Solomon T, Sudlow
924 C, Swann OV, Turtle L, Openshaw PJM, Baillie JK, Semple MG, Noursadeghi M,
925 ISARIC4C Investigators. 2021. Development and validation of the ISARIC 4C
926 Deterioration model for adults hospitalised with COVID-19: a prospective cohort
927 study. *Lancet Respir Med*. doi:10.1016/S2213-2600 (20)30559-2
928 Hashimshony T, Senderovich N, Avital G, Klochendler A, de Leeuw Y, Anavy L, Gennert
929 D, Li S, Livak KJ, Rozenblatt-Rosen O, Dor Y, Regev A, Yanai I. 2016. CEL-Seq2:
930 sensitive highly-multiplexed single-cell RNA-Seq. *Genome Biol* **17**:77.
931 He J, Guo Y, Mao R, Zhang J. 2021. Proportion of asymptomatic coronavirus disease
932 2019: A systematic review and meta-analysis. *J Med Virol* **93**:820–830.
933 Heald-Sargent T, Muller WJ, Zheng X, Rippe J, Patel AB, Kociolek LK. 2020. Age-Related
934 Differences in Nasopharyngeal Severe Acute Respiratory Syndrome Coronavirus
935 2 (SARS-CoV-2) Levels in Patients With Mild to Moderate Coronavirus Disease
936 2019 (COVID-19). *JAMA Pediatr* **174**:902–903.

937 Huang C, Wang Y, Li X, Ren L, Zhao J, Hu Y, Zhang L, Fan G, Xu J, Gu X, Cheng Z, Yu
938 T, Xia J, Wei Y, Wu W, Xie X, Yin W, Li H, Liu M, Xiao Y, Gao H, Guo L, Xie J,
939 Wang G, Jiang R, Gao Z, Jin Q, Wang J, Cao B. 2020. Clinical features of patients
940 infected with 2019 novel coronavirus in Wuhan, China. *Lancet* **395**:497–506.
941 Huang I, Pranata R. 2020. Lymphopenia in severe coronavirus disease-2019 (COVID-
942 19): systematic review and meta-analysis. *J Intensive Care Med* **8**:36.
943 Jamieson AM, Pasman L, Yu S, Gamradt P, Homer RJ, Decker T, Medzhitov R. 2013.
944 Role of tissue protection in lethal respiratory viral-bacterial coinfection. *Science*
945 **340**:1230–1234.
946 Jhaveri KA, Trammell RA, Toth LA. 2007. Effect of environmental temperature on sleep,
947 locomotor activity, core body temperature and immune responses of C57BL/6J
948 mice. *Brain Behav Immun* **21**:975–987.
949 Jones TC, Biele G, Mühlemann B, Veith T, Schneider J, Beheim-Schwarzbach J, Bleicker
950 T, Tesch J, Schmidt ML, Sander LE, Kurth F, Menzel P, Schwarzer R, Zuchowski
951 M, Hofmann J, Krumbholz A, Stein A, Edelmann A, Corman VM, Drosten C. 2021.
952 Estimating infectiousness throughout SARS-CoV-2 infection course. *Science*
953 **373**:eabi5273.
954 Karlberg J. 2004. Do Men Have a Higher Case Fatality Rate of Severe Acute Respiratory
955 Syndrome than Women Do? *American Journal of Epidemiology*.
956 doi:10.1093/aje/kwh056
957 Kassambara A. 2020. ggpubr: “ggplot2” Based Publication Ready Plots.
958 Klein SL, Flanagan KL. 2016. Sex differences in immune responses. *Nat Rev Immunol*
959 **16**:626–638.

960 Klose CSN, Artis D. 2016. Innate lymphoid cells as regulators of immunity, inflammation
961 and tissue homeostasis. *Nat Immunol* **17**:765–774.
962 Kløverpris HN, Kazer SW, Mjösberg J, Mabuka JM, Wellmann A, Ndhlovu Z, Yadon MC,
963 Nhamoyebonde S, Muenchhoff M, Simoni Y, Andersson F, Kuhn W, Garrett N,
964 Burgers WA, Kamya P, Pretorius K, Dong K, Moodley A, Newell EW, Kasprowicz
965 V, Abdool Karim SS, Goulder P, Shalek AK, Walker BD, Ndung'u T, Leslie A. 2016.
966 Innate Lymphoid Cells Are Depleted Irreversibly during Acute HIV-1 Infection in
967 the Absence of Viral Suppression. *Immunity* **44**:391–405.
968 Kompaniyets L. 2021. Body Mass Index and Risk for COVID-19–Related Hospitalization,
969 Intensive Care Unit Admission, Invasive Mechanical Ventilation, and Death —
970 United States, March–December 2020. *MMWR Morb Mortal Wkly Rep* **70**.
971 doi:10.15585/mmwr.mm7010e4
972 Kuri-Cervantes L, Pampena MB, Meng W, Rosenfeld AM, Ittner CAG, Weisman AR,
973 Agyekum RS, Mathew D, Baxter AE, Vella LA, Kuthuru O, Apostolidis SA, Bershaw
974 L, Dougherty J, Greenplate AR, Pattekar A, Kim J, Han N, Gouma S, Weirick ME,
975 Arevalo CP, Bolton MJ, Goodwin EC, Anderson EM, Hensley SE, Jones TK,
976 Mangalmurti NS, Luning Prak ET, Wherry EJ, Meyer NJ, Betts MR. 2020.
977 Comprehensive mapping of immune perturbations associated with severe COVID-
978 19. *Sci Immunol* **5**:eabd7114.
979 Kuznetsova A, Brockhoff PB, Christensen RHB, Others. 2017. lmerTest package: tests
980 in linear mixed effects models. *J Stat Softw* **82**:1–26.

981 Laxminarayan R, Wahl B, Dudala SR, Gopal K, Mohan B C, Neelima S, Jawahar Reddy
982 KS, Radhakrishnan J, Lewnard JA. 2020. Epidemiology and transmission
983 dynamics of COVID-19 in two Indian states. *Science* **370**:691–697.
984 Lee S, Kim T, Lee E, Lee C, Kim H, Rhee H, Park SY, Son H-J, Yu S, Park JW, Choo EJ,
985 Park S, Loeb M, Kim TH. 2020. Clinical Course and Molecular Viral Shedding
986 Among Asymptomatic and Symptomatic Patients With SARS-CoV-2 Infection in a
987 Community Treatment Center in the Republic of Korea. *JAMA Internal Medicine*
988 **180**:1447.
989 Leist SR, Dinnon KH 3rd, Schäfer A, Tse LV, Okuda K, Hou YJ, West A, Edwards CE,
990 Sanders W, Fritch EJ, Gully KL, Scobey T, Brown AJ, Sheahan TP, Moorman NJ,
991 Boucher RC, Gralinski LE, Montgomery SA, Baric RS. 2020. A Mouse-Adapted
992 SARS-CoV-2 Induces Acute Lung Injury and Mortality in Standard Laboratory
993 Mice. *Cell* **183**:1070-1085.e12.
994 Lennon NJ, Bhattacharyya RP, Mina MJ, Rehm HL, Hung DT, Smole S, Woolley A,
995 Lander ES, Gabriel SB. 2021. Cross-sectional assessment of SARS-CoV-2 viral
996 load by symptom status in Massachusetts congregate living facilities. *J Infect Dis*.
997 doi:10.1093/infdis/jiab367
998 Lennon NJ, Bhattacharyya RP, Mina MJ, Rehm HL, Hung DT, Smole S, Woolley A,
999 Lander ES, Gabriel SB. 2020. Comparison of viral levels in individuals with or
1000 without symptoms at time of COVID-19 testing among 32,480 residents and staff
1001 of nursing homes and assisted living facilities in Massachusetts. *bioRxiv*.
1002 doi:10.1101/2020.07.20.20157792
1003 Lenth R. 2020. emmeans: Estimated Marginal Means, aka Least-Squares Means.

1004 Li B, Dewey CN. 2011. RSEM: accurate transcript quantification from RNA-Seq data with
1005 or without a reference genome. *BMC Bioinformatics* **12**:323.
1006 Li B, Zhang S, Zhang R, Chen X, Wang Y, Zhu C. 2020. Epidemiological and Clinical
1007 Characteristics of COVID-19 in Children: A Systematic Review and Meta-Analysis.
1008 *Front Pediatr* **8**:591132.
1009 Licciardi F, Pruccoli G, Denina M, Parodi E, Taglietto M, Rosati S, Montin D. 2020. SARS-
1010 CoV-2-Induced Kawasaki-Like Hyperinflammatory Syndrome: A Novel COVID
1011 Phenotype in Children. *Pediatrics*. doi:10.1542/peds.2020-1711
1012 López-Otín C, Kroemer G. 2021. Hallmarks of Health. *Cell* **184**:33–63.
1013 LoTempio JE, Billings EA, Draper K, Ralph C, Moshgriz M, Duong N, Bard JD, Gai X,
1014 Wessel D, DeBiasi RL, Campos JM, Vilain E, Delaney M, Michael DG. 2021. Novel
1015 SARS-CoV-2 spike variant identified through viral genome sequencing of the
1016 pediatric Washington D.C. COVID-19 outbreak. *medRxiv* 2021.02.08.21251344.
1017 Love M, Anders S, Huber W. 2014. Differential analysis of count data--the DESeq2
1018 package. *Genome Biol* **15**:550.
1019 Lu X, Zhang L, Du H, Zhang J, Li YY, Qu J, Zhang W, Wang Y, Bao S, Li Y, Wu C, Liu H,
1020 Liu D, Shao J, Peng X, Yang Y, Liu Z, Xiang Y, Zhang F, Silva RM, Pinkerton KE,
1021 Shen K, Xiao H, Xu S, Wong GWK, Chinese Pediatric Novel Coronavirus Study
1022 Team. 2020. SARS-CoV-2 Infection in Children. *N Engl J Med* **382**:1663–1665.
1023 Lucas C, Wong P, Klein J, Castro TBR, Silva J, Sundaram M, Ellingson MK, Mao T, Oh
1024 JE, Israelow B, Takahashi T, Tokuyama M, Lu P, Venkataraman A, Park A,
1025 Mohanty S, Wang H, Wyllie AL, Vogels CBF, Earnest R, Lapidus S, Ott IM, Moore
1026 AJ, Muenker MC, Fournier JB, Campbell M, Odio CD, Casanovas-Massana A,

1027 Yale IMPACT Team, Herbst R, Shaw AC, Medzhitov R, Schulz WL, Grubaugh ND,
1028 Dela Cruz C, Farhadian S, Ko AI, Omer SB, Iwasaki A. 2020. Longitudinal
1029 analyses reveal immunological misfiring in severe COVID-19. *Nature* **584**:463–
1030 469.
1031 Luo X, Zhou W, Yan X, Guo T, Wang B, Xia H, Ye L, Xiong J, Jiang Z, Liu Y, Zhang B,
1032 Yang W. 2020. Prognostic Value of C-Reactive Protein in Patients With
1033 Coronavirus 2019. *Clin Infect Dis* **71**:2174–2179.
1034 Márquez EJ, Chung C-H, Marches R, Rossi RJ, Nehar-Belaid D, Eroglu A, Mellert DJ,
1035 Kuchel GA, Banchereau J, Ucar D. 2020. Sexual-dimorphism in human immune
1036 system aging. *Nat Commun* **11**:751.
1037 Mathew D, Giles JR, Baxter AE, Oldridge DA, Greenplate AR, Wu JE, Alanio C, Kuri-
1038 Cervantes L, Pampena MB, D'Andrea K, Manne S, Chen Z, Huang YJ, Reilly JP,
1039 Weisman AR, Ittner CAG, Kuthuru O, Dougherty J, Nzingha K, Han N, Kim J,
1040 Pattekar A, Goodwin EC, Anderson EM, Weirick ME, Gouma S, Arevalo CP,
1041 Bolton MJ, Chen F, Lacey SF, Ramage H, Cherry S, Hensley SE, Apostolidis SA,
1042 Huang AC, Vella LA, UPenn COVID Processing Unit, Betts MR, Meyer NJ, Wherry
1043 EJ. 2020. Deep immune profiling of COVID-19 patients reveals distinct
1044 immunotypes with therapeutic implications. *Science* **369**.
1045 doi:10.1126/science.abc8511
1046 Mauvais-Jarvis F. 2020. Aging, Male Sex, Obesity, and Metabolic Inflammation Create
1047 the Perfect Storm for COVID-19. *Diabetes* **69**:1857–1863.
1048 McCarville JL, Ayres JS. 2018. Disease tolerance: concept and mechanisms. *Curr Opin*
1049 *Immunol* **50**:88–93.

1050 Medzhitov R, Schneider DS, Soares MP. 2012. Disease tolerance as a defense strategy.
1051 *Science* **335**:936–941.
1052 Monticelli LA, Osborne LC, Noti M, Tran SV, Zaiss DMW, Artis D. 2015. IL-33 promotes
1053 an innate immune pathway of intestinal tissue protection dependent on
1054 amphiregulin–EGFR interactions. *Proc Natl Acad Sci U S A* **112**:10762–10767.
1055 Monticelli LA, Sonnenberg GF, Abt MC, Alenghat T, Ziegler CGK, Doering TA,
1056 Angelosanto JM, Laidlaw BJ, Yang CY, Sathaliyawala T, Kubota M, Turner D,
1057 Diamond JM, Goldrath AW, Farber DL, Collman RG, Wherry EJ, Artis D. 2011.
1058 Innate lymphoid cells promote lung-tissue homeostasis after infection with
1059 influenza virus. *Nat Immunol* **12**:1045–1054.
1060 Mudd PA, Crawford JC, Turner JS, Souquette A, Reynolds D, Bender D, Bosanquet JP,
1061 Anand NJ, Striker DA, Martin RS, Boon ACM, House SL, Remy KE, Hotchkiss RS,
1062 Presti RM, O'Halloran JA, Powderly WG, Thomas PG, Ellebedy AH. 2020. Distinct
1063 inflammatory profiles distinguish COVID-19 from influenza with limited
1064 contributions from cytokine storm. *Sci Adv* **6**. doi:10.1126/sciadv.abe3024
1065 O'Driscoll M, Ribeiro Dos Santos G, Wang L, Cummings DAT, Azman AS, Paireau J,
1066 Fontanet A, Cauchemez S, Salje H. 2020. Age-specific mortality and immunity
1067 patterns of SARS-CoV-2. *Nature*. doi:10.1038/s41586-020-2918-0
1068 Patin E, Hasan M, Bergstedt J, Rouilly V, Libri V, Urrutia A, Alanio C, Scepanovic P,
1069 Hammer C, Jönsson F, Beitz B, Quach H, Lim YW, Hunkapiller J, Zepeda M,
1070 Green C, Piasecka B, Leloup C, Rogge L, Huetz F, Peguillet I, Lantz O, Fontes M,
1071 Di Santo JP, Thomas S, Fellay J, Duffy D, Quintana-Murci L, Albert ML, Milieu

1072 Intérieur Consortium. 2018. Natural variation in the parameters of innate immune
1073 cells is preferentially driven by genetic factors. *Nat Immunol* **19**:302–314.
1074 Peckham H, de Gruijter NM, Raine C, Radziszewska A, Ciurtin C, Wedderburn LR,
1075 Rosser EC, Webb K, Deakin CT. 2020. Male sex identified by global COVID-19
1076 meta-analysis as a risk factor for death and ITU admission. *Nature*
1077 *Communications* **11**:6317.
1078 Piasecka B, Duffy D, Urrutia A, Quach H, Patin E, Posseme C, Bergstedt J, Charbit B,
1079 Rouilly V, MacPherson CR, Hasan M, Albaud B, Gentien D, Fellay J, Albert ML,
1080 Quintana-Murci L, Milieu Intérieur Consortium. 2018. Distinctive roles of age, sex,
1081 and genetics in shaping transcriptional variation of human immune responses to
1082 microbial challenges. *Proc Natl Acad Sci U S A* **115**:E488–E497.
1083 Poline J, Gaschignard J, Leblanc C, Madhi F, Foucaud E, Nattes E, Faye A, Bonacorsi
1084 S, Mariani P, Varon E, Smati-Lafarge M, Caseris M, Basmaci R, Lachaume N,
1085 Ouldali N. 2020. Systematic SARS-CoV-2 screening at hospital admission in
1086 children:a French prospective multicenter study. *Clin Infect Dis*.
1087 doi:10.1093/cid/ciaa1044
1088 R Core Team. 2020. R: A Language and Environment for Statistical Computing.
1089 Ra SH, Lim JS, Kim G-U, Kim MJ, Jung J, Kim S-H. 2021. Upper respiratory viral load in
1090 asymptomatic individuals and mildly symptomatic patients with SARS-CoV-2
1091 infection. *Thorax* **76**:61–63.
1092 Råberg L, Sim D, Read AF. 2007. Disentangling genetic variation for resistance and
1093 tolerance to infectious diseases in animals. *Science* **318**:812–814.

1094 Rak GD, Osborne LC, Siracusa MC, Kim BS, Wang K, Bayat A, Artis D, Volk SW. 2016.
1095 IL-33-Dependent Group 2 Innate Lymphoid Cells Promote Cutaneous Wound
1096 Healing. *J Invest Dermatol* **136**:487–496.
1097 Rauber S, Luber M, Weber S, Maul L, Soare A, Wohlfahrt T, Lin N-Y, Dietel K, Bozec A,
1098 Herrmann M, Kaplan MH, Weigmann B, Zaiss MM, Fearon U, Veale DJ, Cañete
1099 JD, Distler O, Rivellese F, Pitzalis C, Neurath MF, McKenzie ANJ, Wirtz S, Schett
1100 G, Distler JHW, Ramming A. 2017. Resolution of inflammation by interleukin-9-
1101 producing type 2 innate lymphoid cells. *Nat Med* **23**:938–944.
1102 Richardson S, Hirsch JS, Narasimhan M, Crawford JM, McGinn T, Davidson KW, the
1103 Northwell COVID-19 Research Consortium, Barnaby DP, Becker LB, Chelico JD,
1104 Cohen SL, Cookingham J, Coppa K, Diefenbach MA, Dominello AJ, Duer-Hefele
1105 J, Falzon L, Gitlin J, Hajizadeh N, Harvin TG, Hirschwerk DA, Kim EJ, Kozel ZM,
1106 Marrast LM, Mogavero JN, Osorio GA, Qiu M, Zanos TP. 2020. Presenting
1107 Characteristics, Comorbidities, and Outcomes Among 5700 Patients Hospitalized
1108 With COVID-19 in the New York City Area. *JAMA* **323**:2052–2059.
1109 Riphagen S, Gomez X, Gonzalez-Martinez C, Wilkinson N, Theocharis P. 2020.
1110 Hyperinflammatory shock in children during COVID-19 pandemic. *Lancet*.
1111 Sanchez KK, Chen GY, Schieber AMP, Redford SE, Shokhirev MN, Leblanc M, Lee YM,
1112 Ayres JS. 2018. Cooperative Metabolic Adaptations in the Host Can Favor
1113 Asymptomatic Infection and Select for Attenuated Virulence in an Enteric
1114 Pathogen. *Cell* **175**:146-158.e15.
1115 Sancho-Shimizu V, Brodin P, Cobat A, Biggs CM, Toubiana J, Lucas CL, Henrickson SE,
1116 Belot A, MIS-C@CHGE, Tangye SG, Milner JD, Levin M, Abel L, Bogunovic D,

1117 Casanova J-L, Zhang S-Y. 2021. SARS-CoV-2–related MIS-C: A key to the viral
1118 and genetic causes of Kawasaki disease? *J Exp Med* **218**.
1119 doi:10.1084/jem.20210446
1120 Schneider DS, Ayres JS. 2008. Two ways to survive infection: what resistance and
1121 tolerance can teach us about treating infectious diseases. *Nature Reviews*
1122 *Immunology* **8**:889–895.
1123 Scully EP, Haverfield J, Ursin RL, Tannenbaum C, Klein SL. 2020. Considering how
1124 biological sex impacts immune responses and COVID-19 outcomes. *Nat Rev*
1125 *Immunol* **20**:442–447.
1126 Solana R, Tarazona R, Gayoso I, Lesur O, Dupuis G, Fulop T. 2012. Innate
1127 immunosenescence: effect of aging on cells and receptors of the innate immune
1128 system in humans. *Semin Immunol* **24**:331–341.
1129 Tesoriero JM, Swain C-AE, Pierce JL, Zamboni L, Wu M, Holtgrave DR, Gonzalez CJ,
1130 Udo T, Morne JE, Hart-Malloy R, Rajulu DT, Leung S-YJ, Rosenberg ES. 2021.
1131 COVID-19 Outcomes Among Persons Living With or Without Diagnosed HIV
1132 Infection in New York State. *JAMA Netw Open* **4**:e2037069.
1133 Verdoni L, Mazza A, Gervasoni A, Martelli L, Ruggeri M, Ciuffreda M, Bonanomi E,
1134 D'Antiga L. 2020. An outbreak of severe Kawasaki-like disease at the Italian
1135 epicentre of the SARS-CoV-2 epidemic: an observational cohort study. *Lancet*
1136 **395**:1771–1778.
1137 Vivier E, Artis D, Colonna M, Diefenbach A, Di Santo JP, Eberl G, Koyasu S, Locksley
1138 RM, McKenzie ANJ, Mebius RE, Powrie F, Spits H. 2018. Innate Lymphoid Cells:
1139 10 Years On. *Cell* **174**:1054–1066.

1140 Wang A, Huen SC, Luan HH, Yu S, Zhang C, Gallezot J-D, Booth CJ, Medzhitov R. 2016.
1141 Opposing Effects of Fasting Metabolism on Tissue Tolerance in Bacterial and Viral
1142 Inflammation. *Cell* **166**:1512-1525.e12.
1143 Wang Y, Lifshitz L, Gellatly K, Vinton CL, Busman-Sahay K, McCauley S, Vangala P, Kim
1144 K, Derr A, Jaiswal S, Kucukural A, McDonel P, Hunt PW, Greenough T, Houghton
1145 J, Somsouk M, Estes JD, Brenchley JM, Garber M, Deeks SG, Luban J. 2020.
1146 HIV-1-induced cytokines deplete homeostatic innate lymphoid cells and expand
1147 TCF7-dependent memory NK cells. *Nat Immunol* **21**:274–286.
1148 Whittaker E, Bamford A, Kenny J, Kaforou M, Jones CE, Shah P, Ramnarayan P, Fraisse
1149 A, Miller O, Davies P, Kucera F, Brierley J, McDougall M, Carter M, Tremoulet A,
1150 Shimizu C, Herberg J, Burns JC, Lyall H, Levin M, PIMS-TS Study Group and
1151 EUCLIDS and PERFORM Consortia. 2020. Clinical Characteristics of 58 Children
1152 With a Pediatric Inflammatory Multisystem Syndrome Temporally Associated With
1153 SARS-CoV-2. *JAMA* **324**:259–269.
1154 Wickham H. 2016. ggplot2: Elegant Graphics for Data Analysis. Springer.
1155 Wickham H, Averick M, Bryan J, Chang W, McGowan L, François R, Grolemund G, Hayes
1156 A, Henry L, Hester J, Kuhn M, Pedersen T, Miller E, Bache S, Müller K, Ooms J,
1157 Robinson D, Seidel D, Spinu V, Takahashi K, Vaughan D, Wilke C, Woo K, Yutani
1158 H. 2019. Welcome to the Tidyverse. *JOSS* **4**:1686.
1159 Yang Q, Monticelli LA, Saenz SA, Chi AW-S, Sonnenberg GF, Tang J, De Obaldia ME,
1160 Bailis W, Bryson JL, Toscano K, Huang J, Haczku A, Pear WS, Artis D, Bhandoola
1161 A. 2013. T cell factor 1 is required for group 2 innate lymphoid cell generation.
1162 *Immunity* **38**:694–704.

1163 Yang Q, Saldi TK, Gonzales PK, Lasda E, Decker CJ, Tat KL, Fink MR, Hager CR, Davis
1164 JC, Ozeroff CD, Muhlrad D, Clark SK, Fattor WT, Meyerson NR, Paige CL,
1165 Gilchrist AR, Barbachano-Guerrero A, Worden-Sapper ER, Wu SS, Brisson GR,
1166 McQueen MB, Dowell RD, Leinwand L, Parker R, Sawyer SL. 2021. Just 2% of
1167 SARS-CoV-2−positive individuals carry 90% of the virus circulating in
1168 communities. *Proc Natl Acad Sci U S A* **118**. doi:10.1073/pnas.2104547118
1169 Yonker LM, Gilboa T, Ogata AF, Senussi Y, Lazarovits R, Boribong BP, Bartsch YC,
1170 Loiselle M, Noval Rivas M, Porritt RA, Lima R, Davis JP, Farkas EJ, Burns MD,
1171 Young N, Mahajan VS, Hajizadeh S, Herrera Lopez XI, Kreuzer J, Morris R,
1172 Martinez EE, Han I, Griswold K Jr, Barry NC, Thompson DB, Church G, Edlow AG,
1173 Haas W, Pillai S, Arditi M, Alter G, Walt DR, Fasano A. 2021. Multisystem
1174 inflammatory syndrome in children is driven by zonulin-dependent loss of gut
1175 mucosal barrier. *J Clin Invest*. doi:10.1172/JCI149633
1176 Yonker LM, Neilan AM, Bartsch Y, Patel AB, Regan J, Arya P, Gootkind E, Park G,
1177 Hardcastle M, St John A, Appleman L, Chiu ML, Fialkowski A, De la Flor D, Lima
1178 R, Bordt EA, Yockey LJ, D'Avino P, Fischinger S, Shui JE, Lerou PH, Bonventre
1179 JV, Yu XG, Ryan ET, Bassett IV, Irimia D, Edlow AG, Alter G, Li JZ, Fasano A.
1180 2020. Pediatric Severe Acute Respiratory Syndrome Coronavirus 2 (SARS-CoV-
1181 2): Clinical Presentation, Infectivity, and Immune Responses. *J Pediatr* **227**:45-
1182 52.e5.
1183 Yu G, Wang L-G, Han Y, He Q-Y. 2012. clusterProfiler: an R Package for Comparing
1184 Biological Themes Among Gene Clusters. *OMICS* **16**:284–287.

1185 Yudanin NA, Schmitz F, Flamar A-L, Thome JJC, Tait Wojno E, Moeller JB, Schirmer M,
1186 Latorre IJ, Xavier RJ, Farber DL, Monticelli LA, Artis D. 2019. Spatial and Temporal
1187 Mapping of Human Innate Lymphoid Cells Reveals Elements of Tissue Specificity.
1188 *Immunity* **50**:505-519.e4.
1189 Yukselen O, Turkyilmaz O, Ozturk AR, Garber M, Kucukural A. 2020. DolphinNext: a
1190 distributed data processing platform for high throughput genomics. *BMC*
1191 *Genomics* **21**:310.
1192 Zhang Z-L, Hou Y-L, Li D-T, Li F-Z. 2020. Laboratory findings of COVID-19: a systematic
1193 review and meta-analysis. *Scand J Clin Lab Invest* **80**:441–447.
1194 Zhao Q, Meng M, Kumar R, Wu Y, Huang J, Deng Y, Weng Z, Yang L. 2020.
1195 Lymphopenia is associated with severe coronavirus disease 2019 (COVID-19)
1196 infections: A systemic review and meta-analysis. *Int J Infect Dis* **96**:131–135.
1197 Zheng M, Gao Y, Wang G, Song G, Liu S, Sun D, Xu Y, Tian Z. 2020. Functional
1198 exhaustion of antiviral lymphocytes in COVID-19 patients. *Cell Mol Immunol*.
1199 Zhou F, Yu T, Du R, Fan G, Liu Y, Liu Z, Xiang J, Wang Y, Song B, Gu X, Guan L, Wei
1200 Y, Li H, Wu X, Xu J, Tu S, Zhang Y, Chen H, Cao B. 2020. Clinical course and risk
1201 factors for mortality of adult inpatients with COVID-19 in Wuhan, China: a
1202 retrospective cohort study. *Lancet* **395**:1054–1062.
1203

1204
1205
1206
1207

1208 **ACKNOWLEDGEMENTS**

1209 We thank the Massachusetts Consortium for Pathogen Readiness Specimen Collection
1210 and Processing Team listed below and members of the Yu and Luban Labs. This work
1211 was supported in part by the Massachusetts Consortium for Pathogen Readiness through
1212 grants from the Evergrande Fund and NIH grants R37AI147868 and R01AI148784 to J.L.
1213 and Ruth L. Kirschstein NRSA Fellowship F30HD100110 to N.J.S. The MGH/MassCPR
1214 COVID biorepository was supported by a gift from Ms. Enid Schwartz, by the Mark and
1215 Lisa Schwartz Foundation, the Massachusetts Consortium for Pathogen Readiness, and
1216 the Ragon Institute of MGH, MIT and Harvard. The Pediatric COVID-19 Biorepository was
1217 supported by the National Heart, Lung, and Blood Institute (5K08HL143183 to LMY), and
1218 the Department of Pediatrics at Massachusetts General Hospital *for* Children (to LMY).

1219

1220 MGH COVID-19 Collection & Processing Team participants Collection Team:
1221 Kendall Lavin-Parsons[1], Blair Parry[1], Brendan Lilley[1], Carl Lodenstein[1], Brenna McKaig[1],
1222 Nicole Charland[1], Hargun Khanna[1], Justin Margolin[1]
1223 Processing Team: Anna Gonye[2], Irena Gushterova[2], Tom Lasalle[2], Nihaarika Sharma[2],
1224 Brian C. Russo[3], Maricarmen Rojas-Lopez[3], Moshe Sade-Feldman[4], Kasidet
1225 Manakongtreecheep[4], Jessica Tantivit[4], Molly Fisher Thomas[4]
1226 Massachusetts Consortium on Pathogen Readiness: Betelihem A. Abayneh[5], Patrick
1227 Allen[5], Diane Antille[5], Katrina Armstrong[5], Siobhan Boyce[5], Joan Braley[5], Karen Branch[5],
1228 Katherine Broderick[5], Julia Carney[5], Andrew Chan[5], Susan Davidson[5], Michael Dougan[5],
1229 David Drew[5], Ashley Elliman[5], Keith Flaherty[5], Jeanne Flannery[5], Pamela Forde[5], Elise
1230 Gettings[5], Amanda Griffin[5], Sheila Grimmel[5], Kathleen Grinke[5], Kathryn Hall[5], Meg

1231 Healy[5], Deborah Henault[5], Grace Holland[5], Chantal Kayitesi[5], Vlasta LaValle[5], Yuting Lu[5],
1232 Sarah Luthern[5], Jordan Marchewka (Schneider)[5], Brittani Martino[5], Roseann
1233 McNamara[5], Christian Nambu[5], Susan Nelson[5], Marjorie Noone[5], Christine Ommerborn[5],
1234 Lois Chris Pacheco[5], Nicole Phan[5], Falisha A. Porto[5], Edward Ryan[5], Kathleen Selleck[5],
1235 Sue Slaughenhaupt[5], Kimberly Smith Sheppard[5], Elizabeth Suschana[5], Vivine Wilson[5],
1236 Galit Alter[6], Alejandro Balazs[6], Julia Bals[6], Max Barbash[6], Yannic Bartsch[6], Julie
1237 Boucau[6], Josh Chevalier[6], Fatema Chowdhury[6], Kevin Einkauf[6], Jon Fallon[6], Liz Fedirko[6],
1238 Kelsey Finn[6], Pilar Garcia-Broncano[6], Ciputra Hartana[6], Chenyang Jiang[6], Paulina
1239 Kaplonek[6], Marshall Karpell[6], Evan C. Lam[6], Kristina Lefteri[6], Xiaodong Lian[6], Mathias
1240 Lichterfeld[6], Daniel Lingwood[6], Hang Liu[6], Jinqing Liu[6], Natasha Ly[6], Ashlin Michell[6], Ilan
1241 Millstrom[6], Noah Miranda[6], Claire O'Callaghan[6], Matthew Osborn[6], Shiv Pillai[6], Yelizaveta
1242 Rassadkina[6], Alexandra Reissis[6], Francis Ruzicka[6], Kyra Seiger[6], Libera Sessa[6],
1243 Christianne Sharr[6], Sally Shin[6], Nishant Singh[6], Weiwei Sun[6], Xiaoming Sun[6], Hannah
1244 Ticheli[6], Alicja Trocha-Piechocka[6], Daniel Worrall[6], Alex Zhu[6], George Daley[7], David
1245 Golan[7], Howard Heller[7], Arlene Sharpe[7], Nikolaus Jilg[8], Alex Rosenthal[8], Colline Wong[8]
1246
1247 [1]Department of Emergency Medicine, Massachusetts General Hospital, Boston, MA,
1248 USA.
1249 [2]Massachusetts General Hospital Cancer Center, Boston, MA, USA.
1250 [3]Division of Infectious Diseases, Department of Medicine, Massachusetts General
1251 Hospital, Boston, MA, USA.
1252 [4]Massachusetts General Hospital Center for Immunology and Inflammatory Diseases,
1253 Boston, MA, USA.

1254 [5]Massachusetts General Hospital, Boston, MA, USA.

1255 [6]Ragon Institute of MGH, MIT and Harvard, Cambridge, MA, USA.

1256 [7]Harvard Medical School, Boston, MA, USA.

1257 [8]Brigham and Women's Hospital, Boston, MA, USA.

1258

1259 **Author information**

1260 Correspondence and requests for materials should be addressed to J.L.

1261 (jeremy.luban@umassmed.edu).